Planck Swift and Fermi simultaneous observations of blazars

Simultaneous *Planck*, *Swift*, and *Fermi* observations of X-ray and γ-ray selected blazars

P. Giommi[2,3], G. Polenta[2,23], A. Lähteenmäki[1,19], D. J. Thompson[5], M. Capalbi[2], S. Cutini[2], D. Gasparrini[2], J. González-Nuevo[43], J. León-Tavares[1], M. López-Caniego[32], M. N. Mazziotta[33], C. Monte[14,33], M. Perri[2], S. Rainò[14,33], G. Tosti[35,15], A. Tramacere[28], F. Verrecchia[2], H. D. Aller[4], M. F. Aller[4], E. Angelakis[41], D. Bastieri[13,34], A. Berdyugin[45], A. Bonaldi[37], L. Bonavera[43,7], C. Burigana[26], D. N. Burrows[10], S. Buson[34], E. Cavazzuti[2], G. Chincarini[46], S. Colafrancesco[23], L. Costamante[47], F. Cuttaia[26], F. D'Ammando[27], G. de Zotti[22,43], M. Frailis[24], L. Fuhrmann[41], S. Galeotta[24], F. Gargano[33], N. Gehrels[5], N. Giglietto[14,33], F. Giordano[14], M. Giroletti[25], E. Keihänen[12], O. King[42], T. P. Krichbaum[41], A. Lasenby[6,38], N. Lavonen[1], C. R. Lawrence[36], C. Leto[2], E. Lindfors[45], N. Mandolesi[26], M. Massardi[22], W. Max-Moerbeck[42], P. F. Michelson[47], M. Mingaliev[44], P. Natoli[16,2,26], I. Nestoras[41], E. Nieppola[1,17], K. Nilsson[17], B. Partridge[18], V. Pavlidou[42], T. J. Pearson[8,29], P. Procopio[26], J. P. Rachen[40], A. Readhead[42], R. Reeves[42], A. Reimer[31,47], R. Reinthal[45], S. Ricciardi[26], J. Richards[42], D. Riquelme[30], J. Saarinen[45], A. Sajina[11], M. Sandri[26], P. Savolainen[1], A. Sievers[30], A. Sillanpää[45], Y. Sotnikova[44], M. Stevenson[42], G. Tagliaferri[21], L. Takalo[45], J. Tammi[1], D. Tavagnacco[24], L. Terenzi[26], L. Toffolatti[9], M. Tornikoski[1], C. Trigilio[20], M. Turunen[1], G. Umana[20], H. Ungerechts[30], F. Villa[26], J. Wu[39], A. Zacchei[24], J. A. Zensus[41], and X. Zhou[39]

A&A 2012, in press ArXiv:1108.1114

Two blazar classes

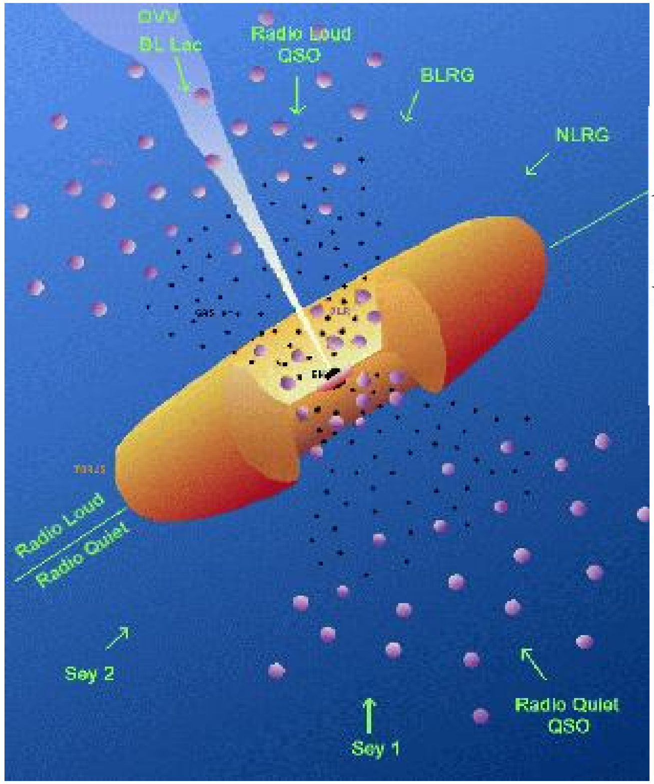

BL Lacs

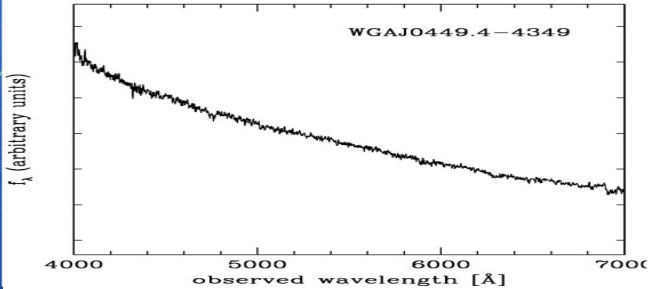

FSRQs

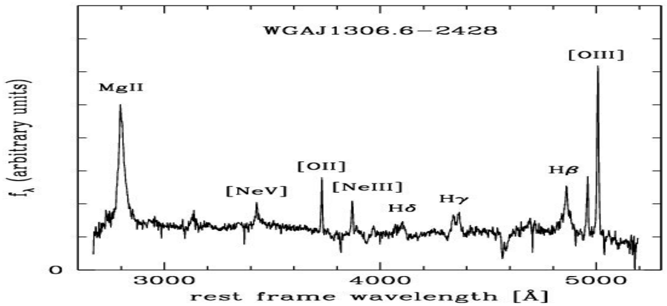

As of today, about 3,060 blazars are known (Bzcat, third edition, Massaro et al. 2011).

FSRQs
BL Lacs

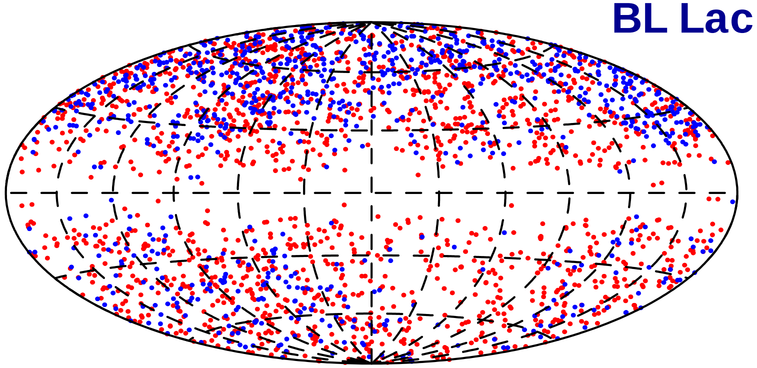

Fermi, Planck, Swift and other facilities (e.g. SDSS, WISE) are increasing this number quickly.

Planck ERCSC catalog: ~550 confirmed blazars and ~130 blazar candidates
ASDC, 2012, in preparation

- **Large number of sources:**
  175 blazars observed by Swift when they were in the FOV of Planck: ~160 Swift ToOs

- **Truly simultaneous Planck Swift Fermi + ground based telescopes**

- **Multi-selection approach. Four flux-limited samples.**
  Soft X-ray (RASS, sample)
  Hard X-ray (Swift-BAT sample)
  γ-ray (Fermi sample)
  Radio (100 brightest northern sources)
- **Fermi-LAT integrations:**
  simultaneous (~1week),
  2 months,
  27 months

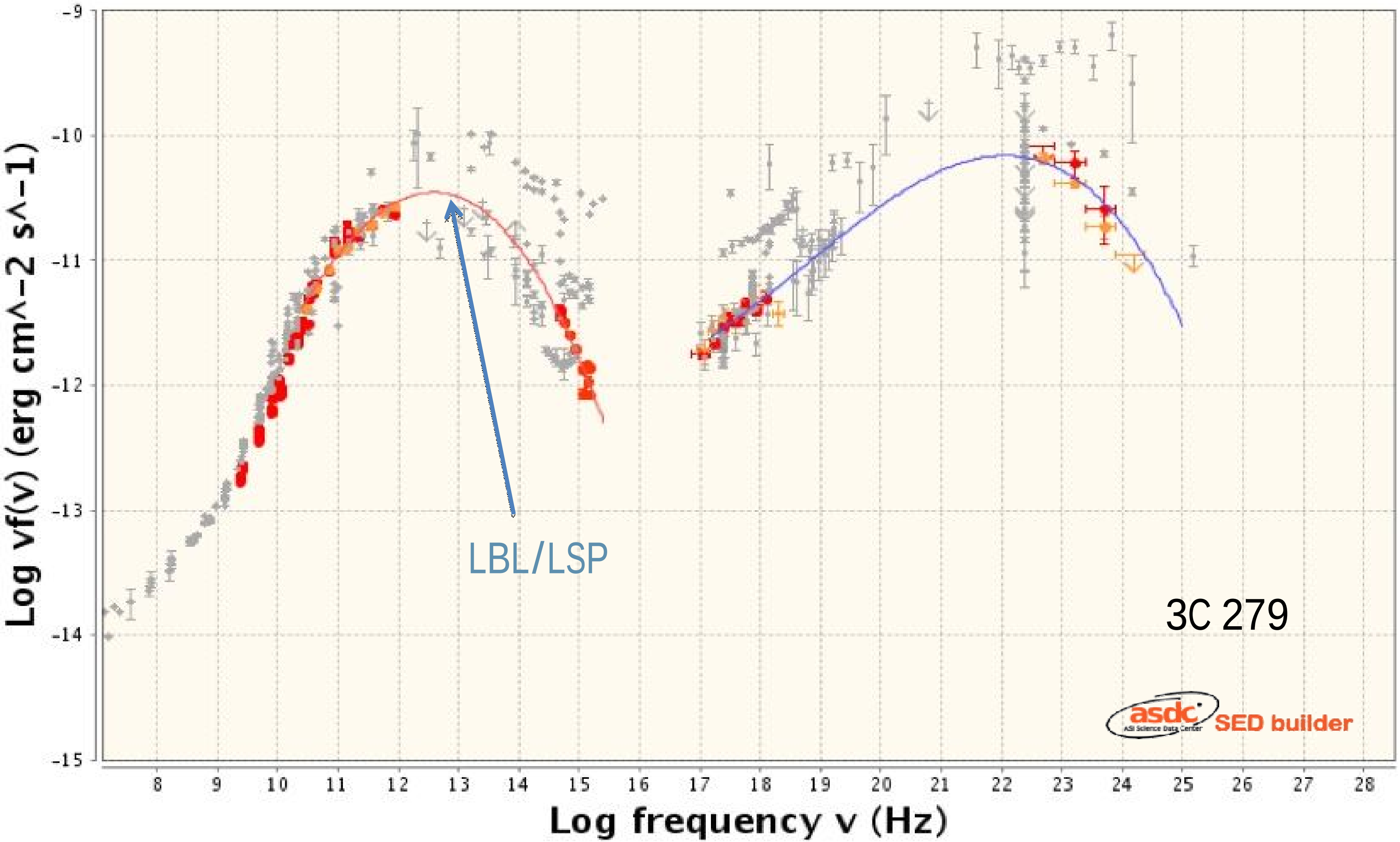
Log vf(v) (erg cm^-2 s^-1)
Log frequency v (Hz)
LBL/LSP
3C 279
SED builder

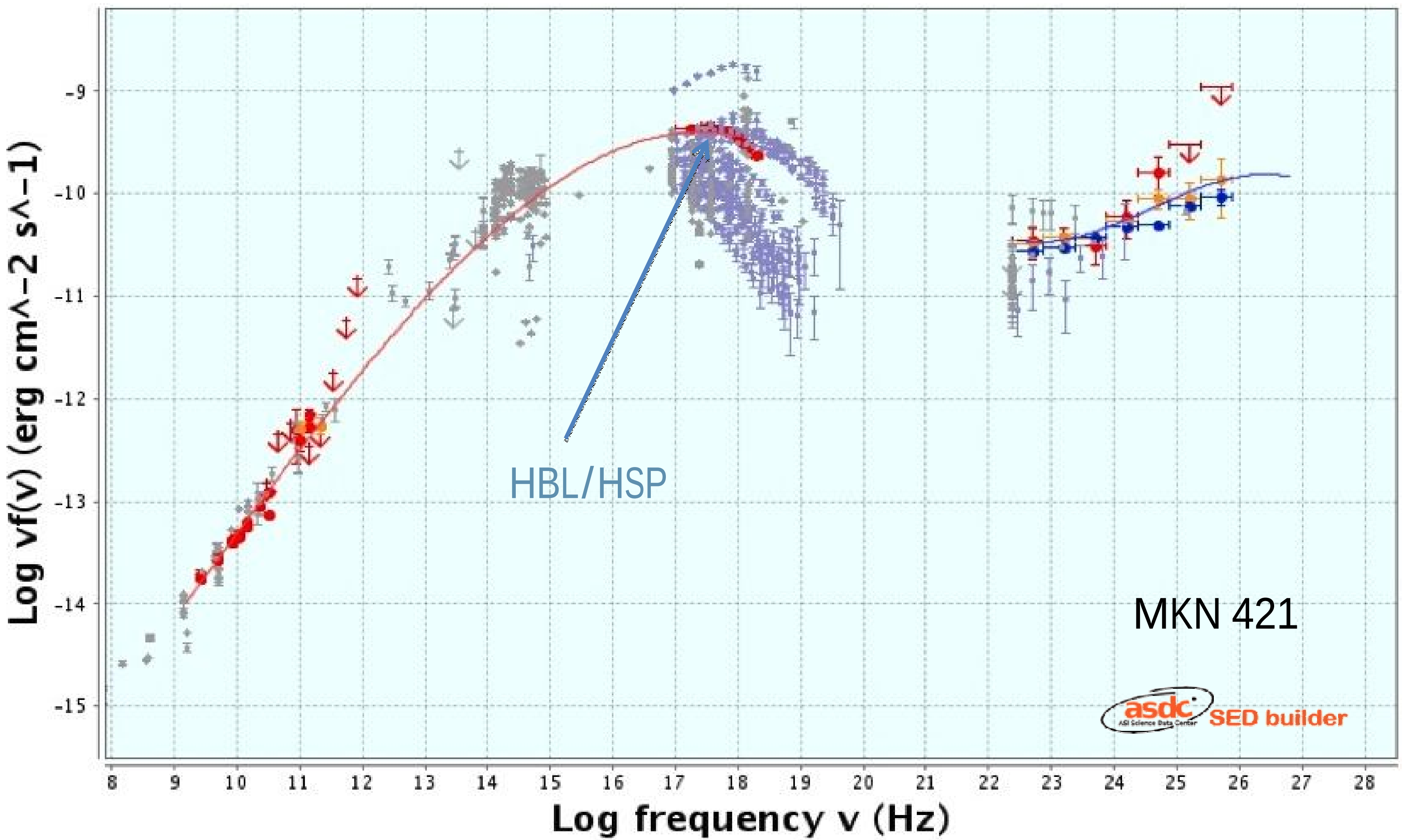

HBL/HSP
MKN 421
SED builder
Log νf(ν) (erg cm^-2 s^-1)
Log frequency ν (Hz)
-9
-10
-11
-12
-13
-14
-15
8 9 10 11 12 13 14 15 16 17 18 19 20 21 22 23 24 25 26 27 28

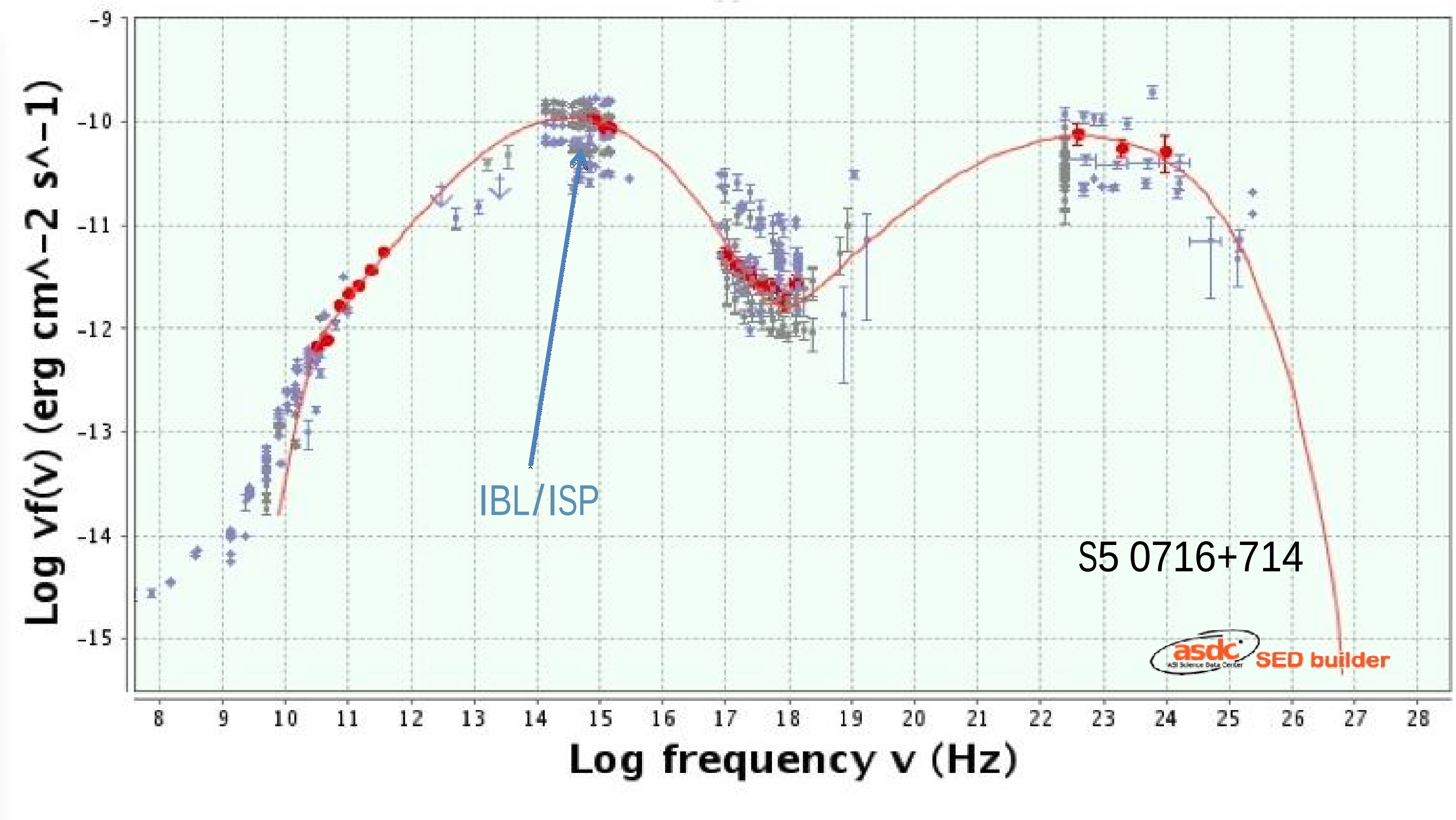

Log νf(ν) (erg cm^-2 s^-1)
Log frequency ν (Hz)
IBL/ISP
S5 0716+714
asdc SED builder

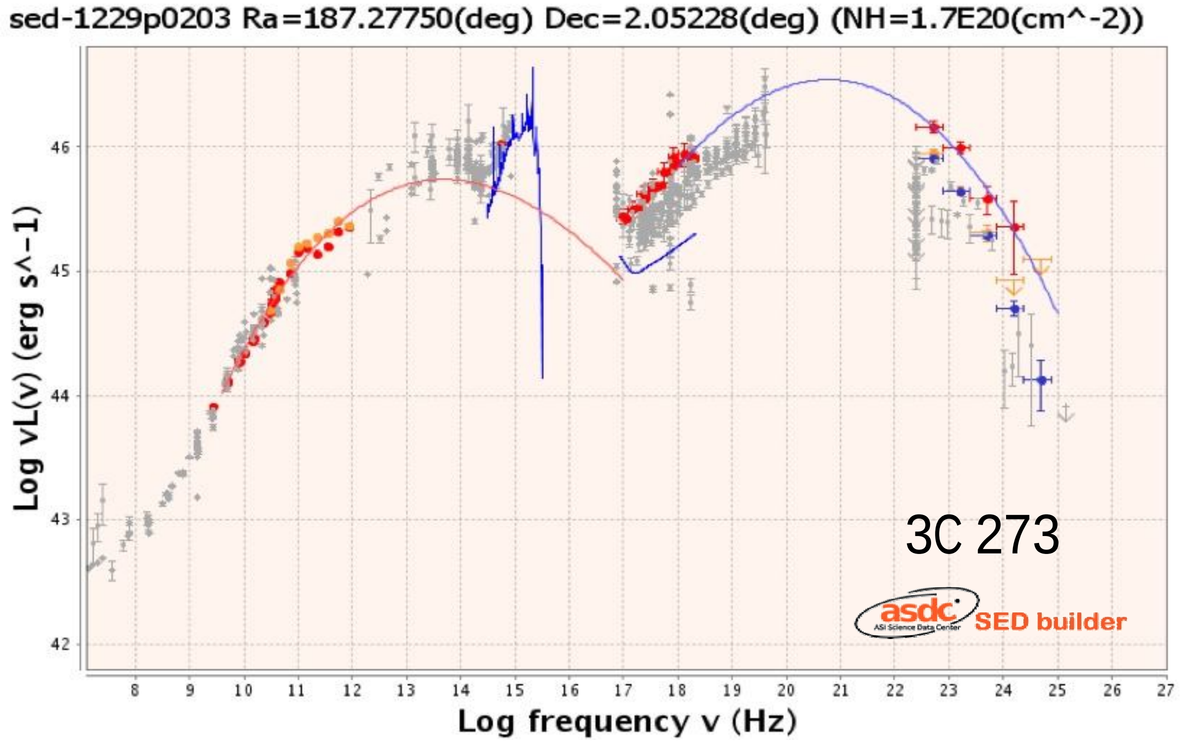
sed-1229p0203 Ra=187.27750(deg) Dec=2.05228(deg) (NH=1.7E20(cm^-2))
Log νL(ν) (erg s^-1)
Log frequency ν (Hz)
3C 273
asdc ASI Science Data Center
SED builder

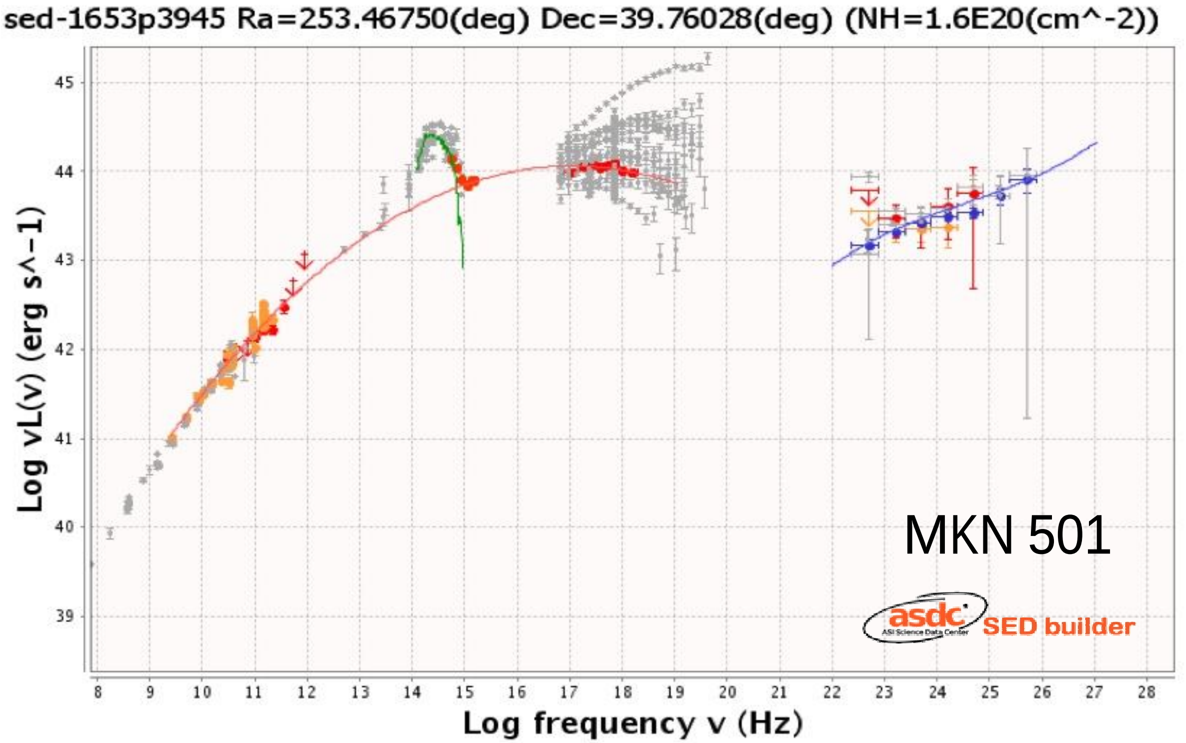
sed-1653p3945 Ra=253.46750(deg) Dec=39.76028(deg) (NH=1.6E20(cm^-2))
Log νL(ν) (erg s^-1)
Log frequency ν (Hz)
MKN 501
asdc ASI Science Data Center
SED builder

Summary of γ-ray detections (TS > 25) in 27 month Fermi-LAT data.

Sample	No. of detected sources		
	FSRQs	BL Lacs	Uncertain
Fermi-LAT	28 (100%)	14 (100%)	8 (100%)
Swift-BAT	17 (63%)	7 (100%)	3 (50%)
Rosat/RASS	[illegible] (53%)	14 (88%)	2 (17%)
Radio	43 (72%)	16 (100%)	9 (64%)

The synchrotron/invC peak frequencies ν_{peak} and intensities $\nu_{peak}\, f(\nu_{peak})$

Measured using 3rd degree polynomial functions

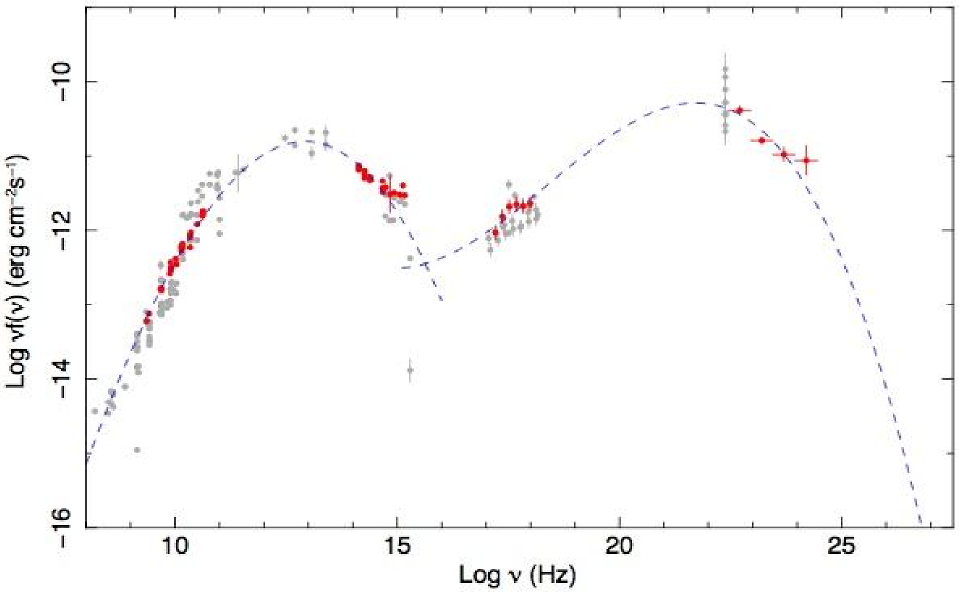

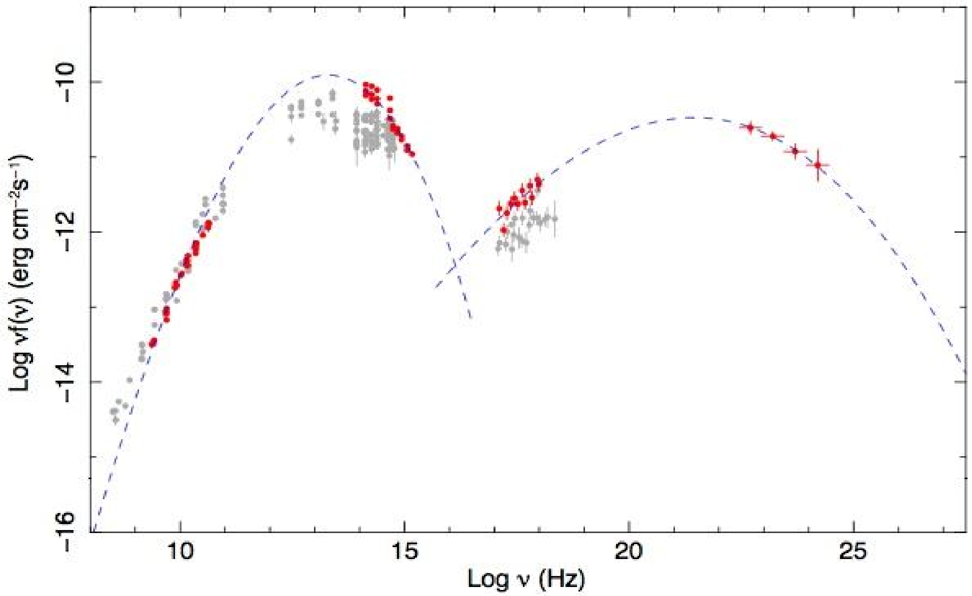

The synchrotron/invC peak frequencies ν_{peak} and intensities $\nu_{peak}\, f(\nu_{peak})$

Measured using 3rd degree polynomial functions

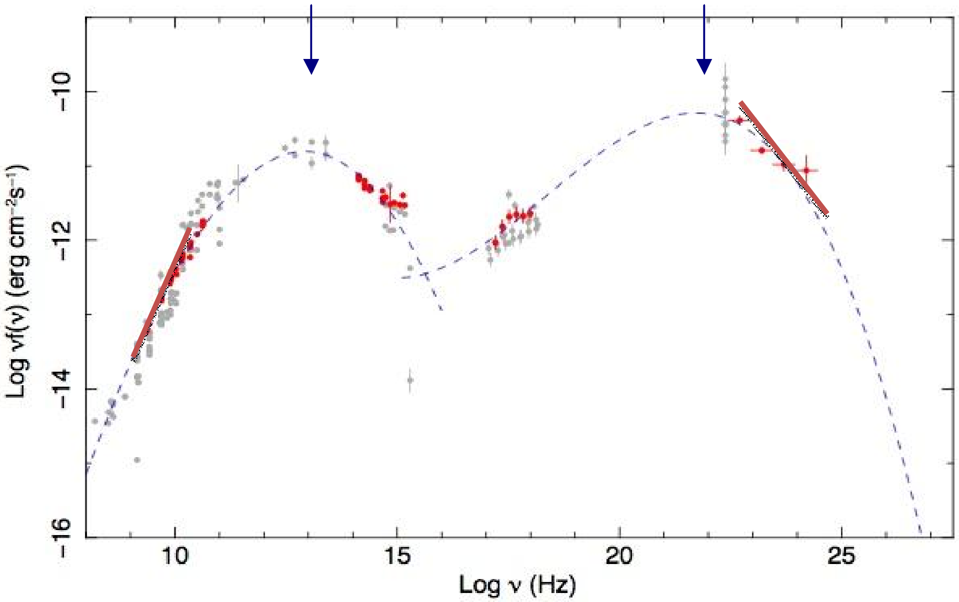

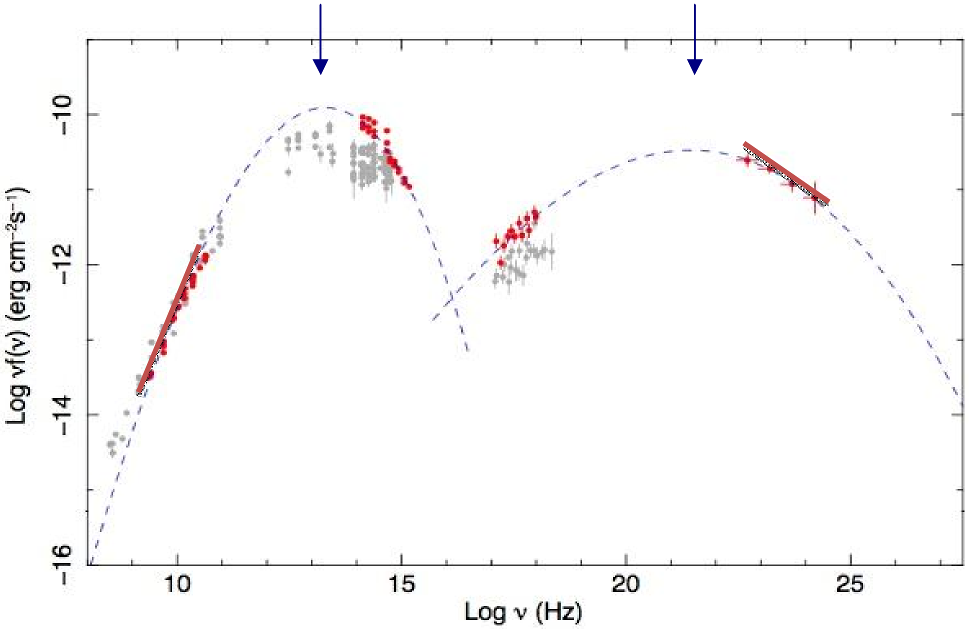

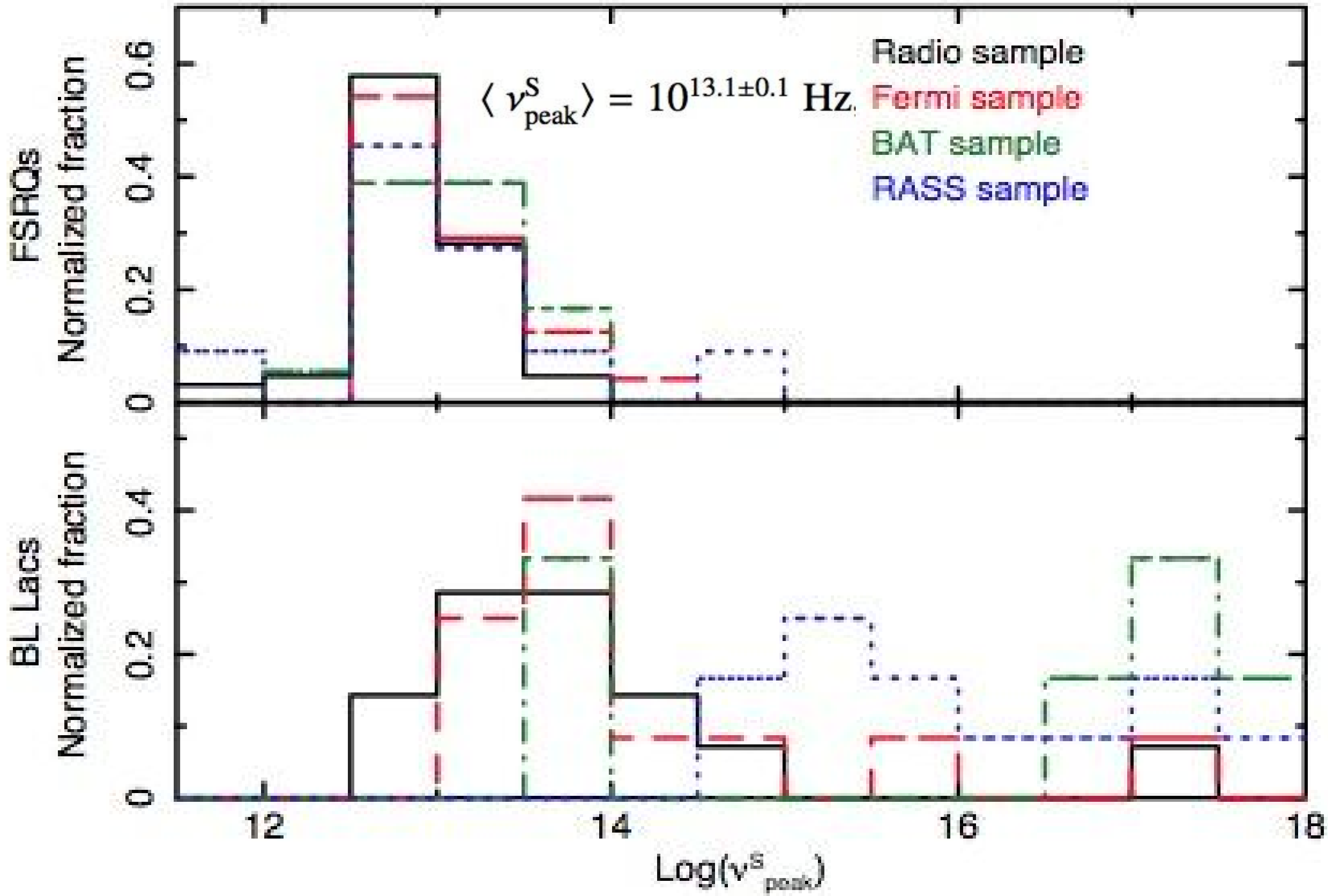

Radio sample
Fermi sample
BAT sample
RASS sample
$\langle \nu^S_{peak} \rangle = 10^{13.1\pm0.1}$ Hz.
FSRQs
Normalized fraction
BL Lacs
Normalized fraction
0
0.2
0.4
0.6
12
14
16
18
Log(ν^S_{peak})

Testing the simplest scenario:
homogeneous SSC

$$\frac{\nu_{peak}^{IC}}{\nu_{peak}^{S}} \simeq \frac{4}{3}(\gamma_{peak}^{SSC})^2$$

(Thomson regime)

$$\gamma_{peak}^{SSC} = \sqrt{3/4 \cdot \nu_{peak}^{IC}/\nu_{peak}^{S}}$$

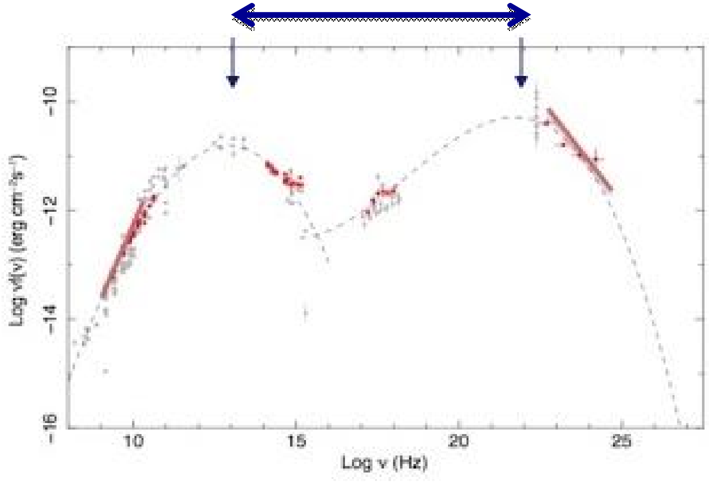

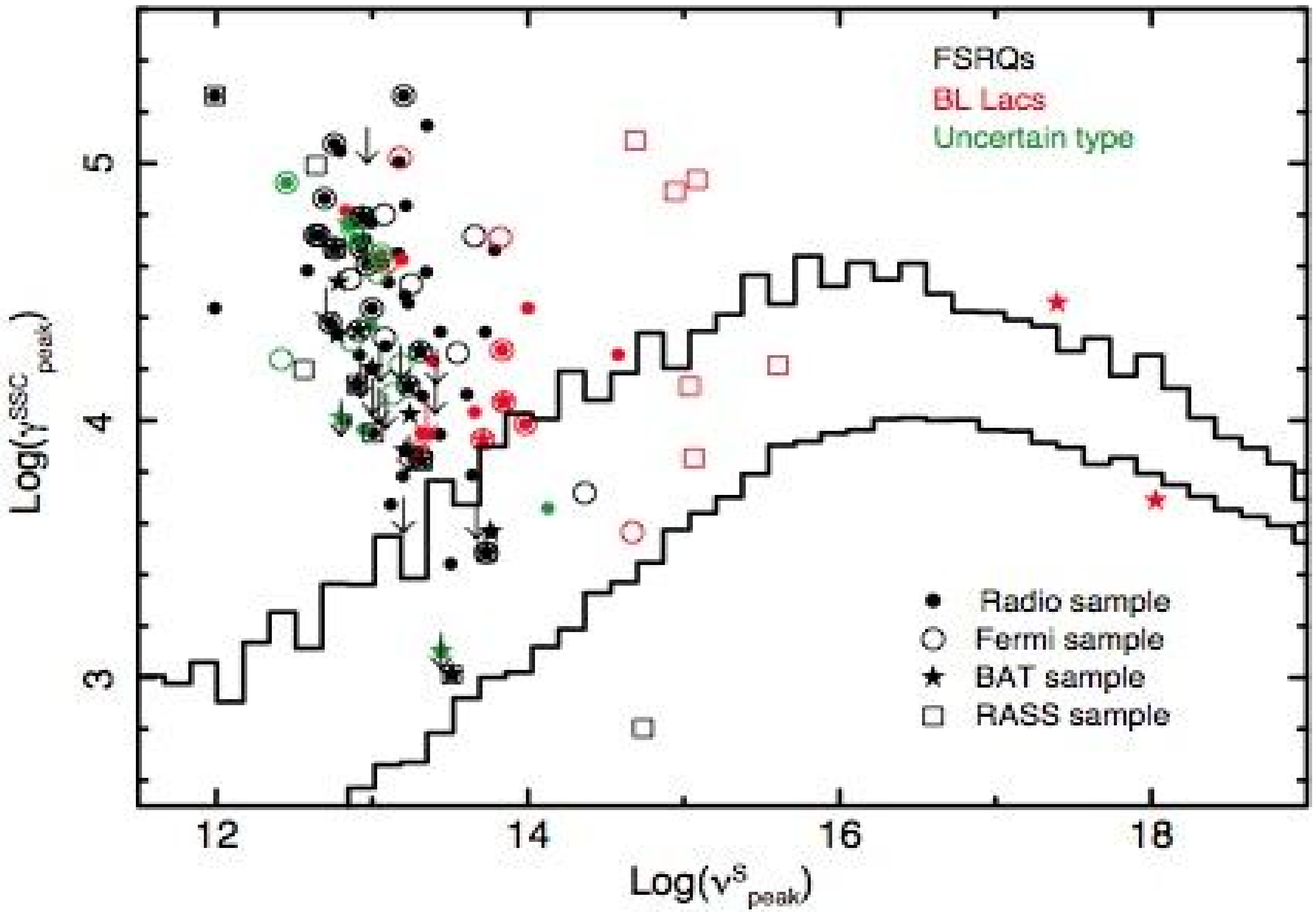
FSRQs
BL Lacs
Uncertain type
Radio sample
Fermi sample
BAT sample
RASS sample
Log(γ^SSC_peak)
Log(ν^S_peak)
3
4
5
12
14
16
18

The Compton dominance

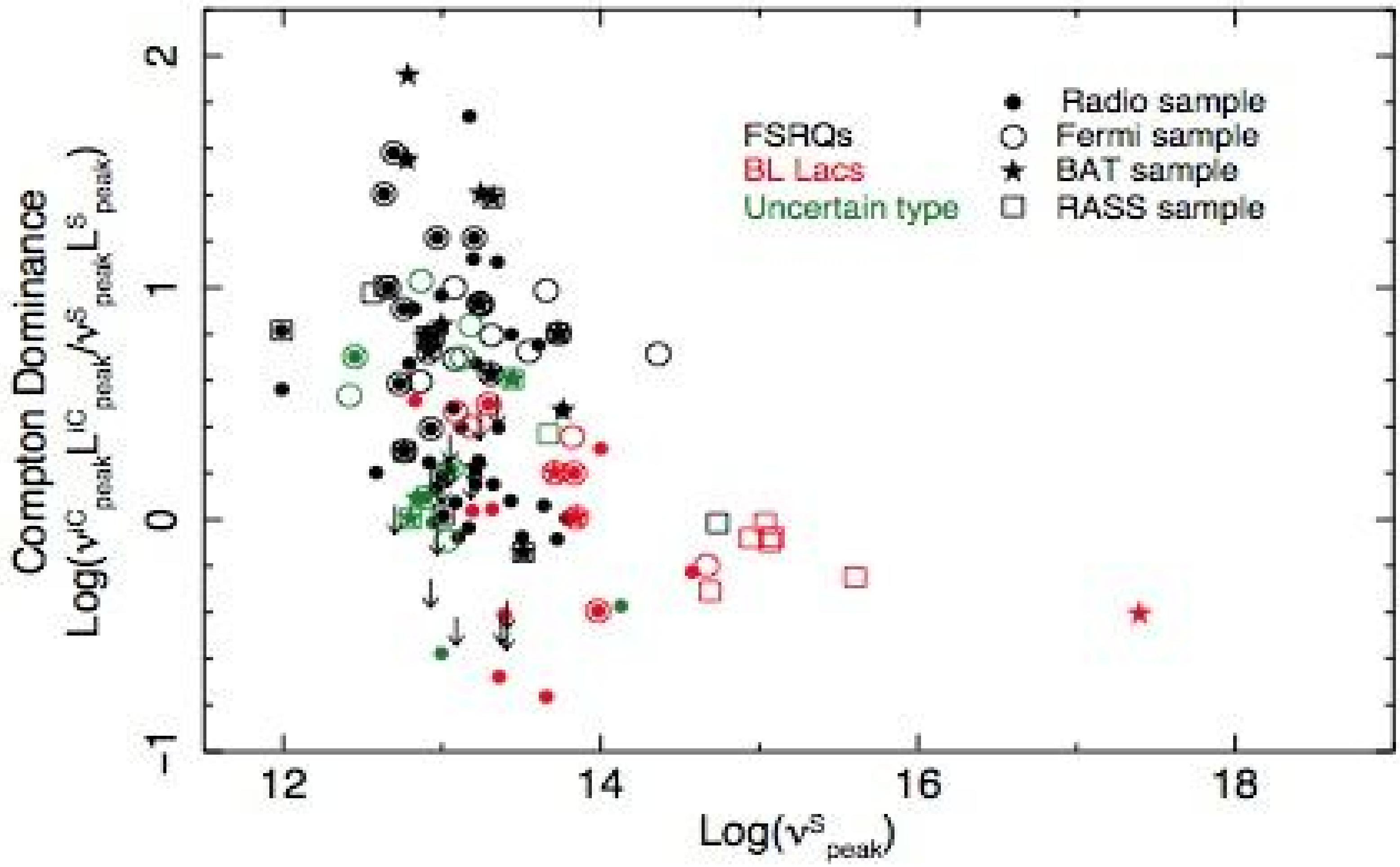

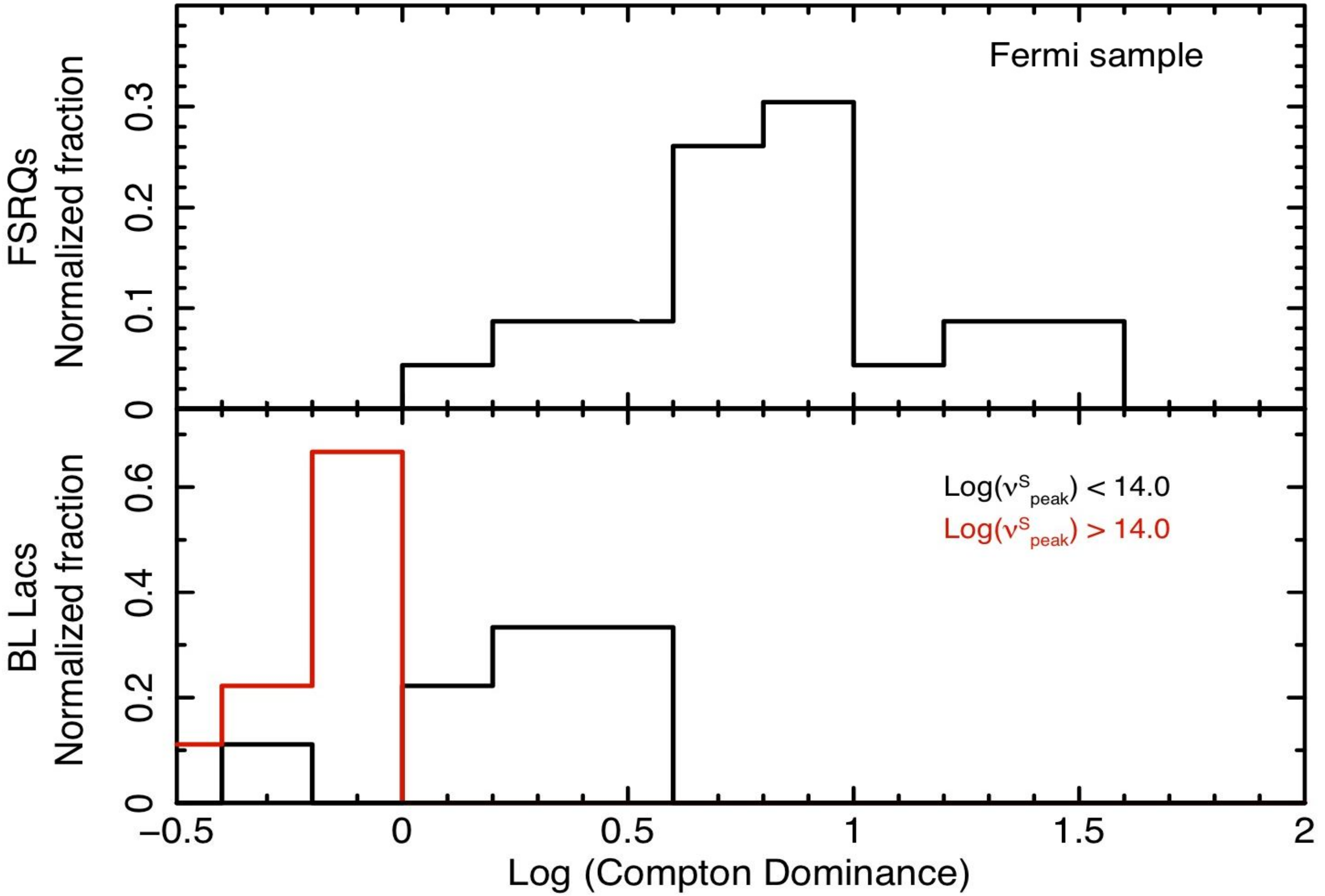
Fermi sample
FSRQs
Normalized fraction
0
0.1
0.2
0.3
BL Lacs
Normalized fraction
0
0.2
0.4
0.6
Log(ν^{S}_{peak}) < 14.0
Log(ν^{S}_{peak}) > 14.0
−0.5
0
0.5
1
1.5
2
Log (Compton Dominance)

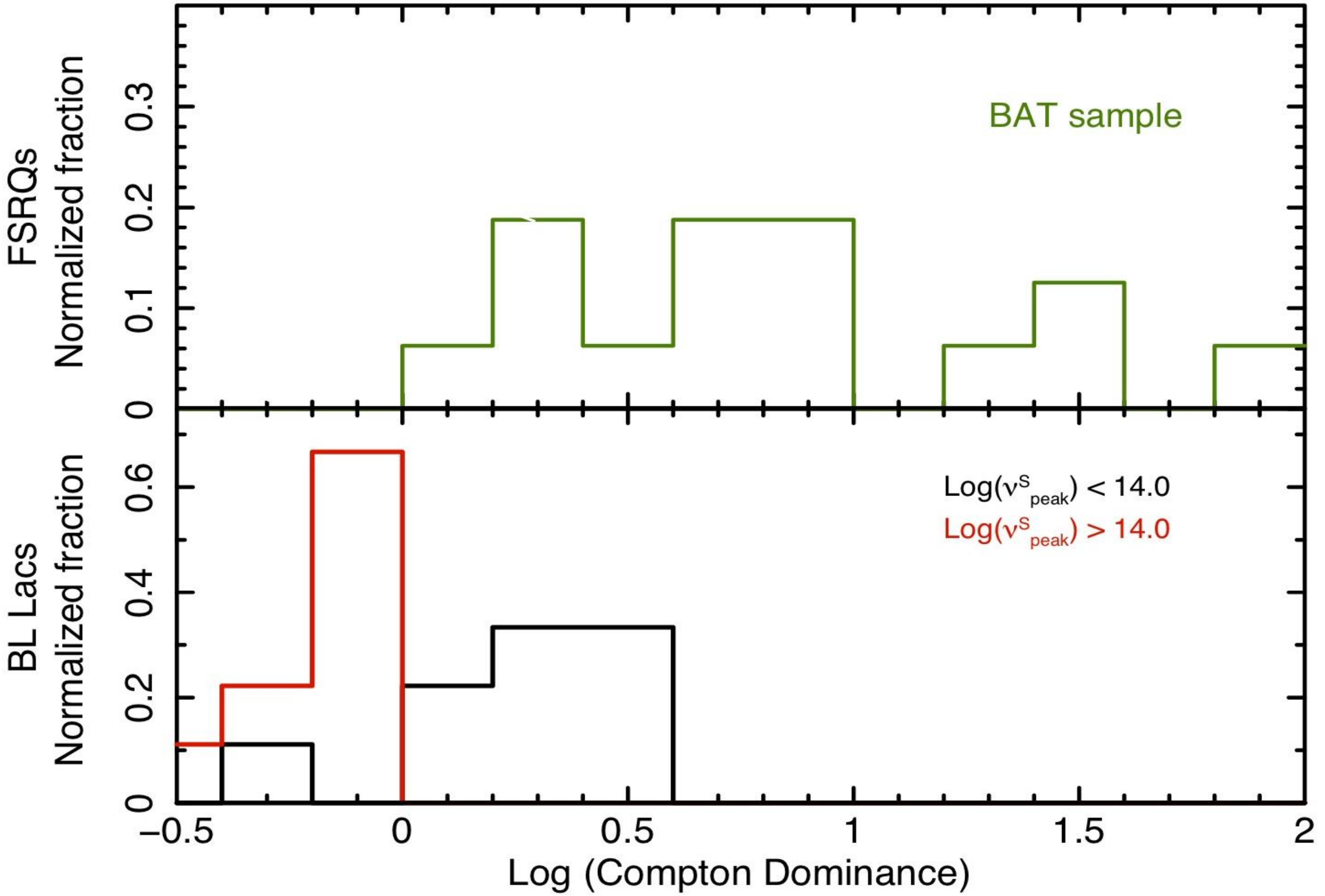

FSRQs
Normalized fraction
BAT sample
BL Lacs
Normalized fraction
Log(ν^S_peak) < 14.0
Log(ν^S_peak) > 14.0
Log (Compton Dominance)

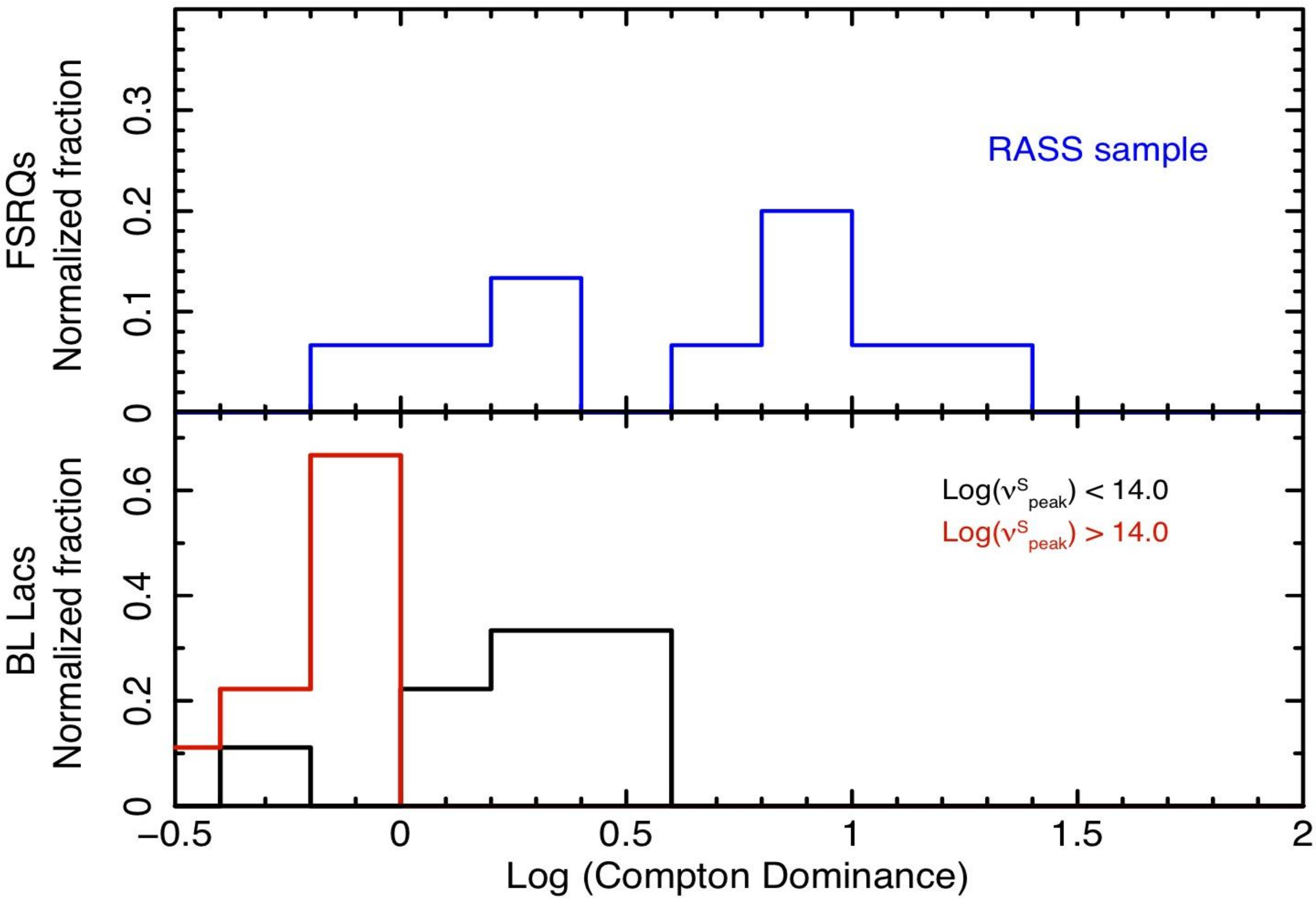

RASS sample
FSRQs
Normalized fraction
BL Lacs
Normalized fraction
Log(ν^{S}_{peak}) < 14.0
Log(ν^{S}_{peak}) > 14.0
Log (Compton Dominance)
0
0.1
0.2
0.3
0.4
0.6
−0.5
0.5
1
1.5
2

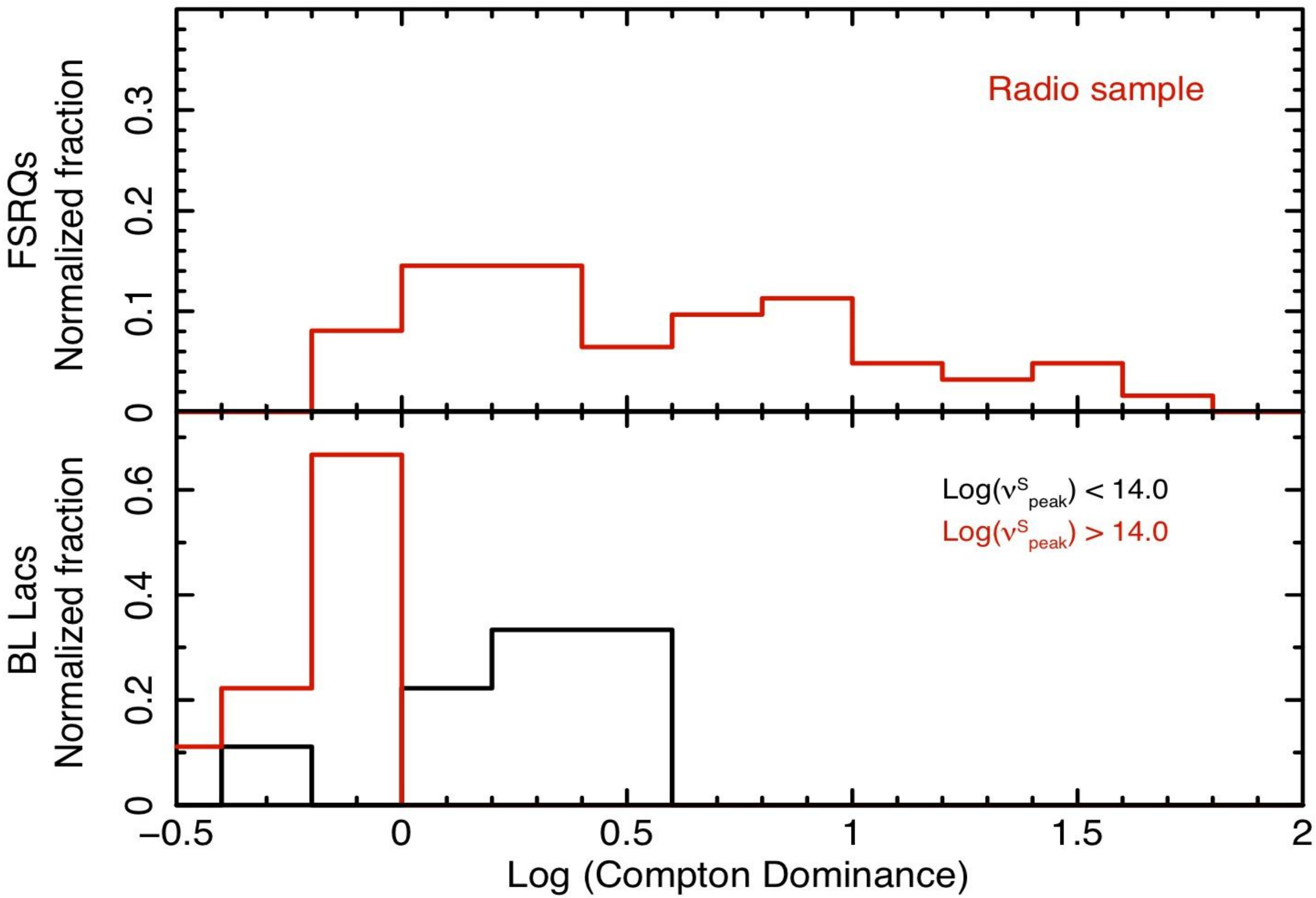

Radio sample
FSRQs
Normalized fraction
0
0.1
0.2
0.3
BL Lacs
Normalized fraction
0
0.2
0.4
0.6
Log(ν^{S}_{peak}) < 14.0
Log(ν^{S}_{peak}) > 14.0
−0.5
0
0.5
1
1.5
2
Log (Compton Dominance)

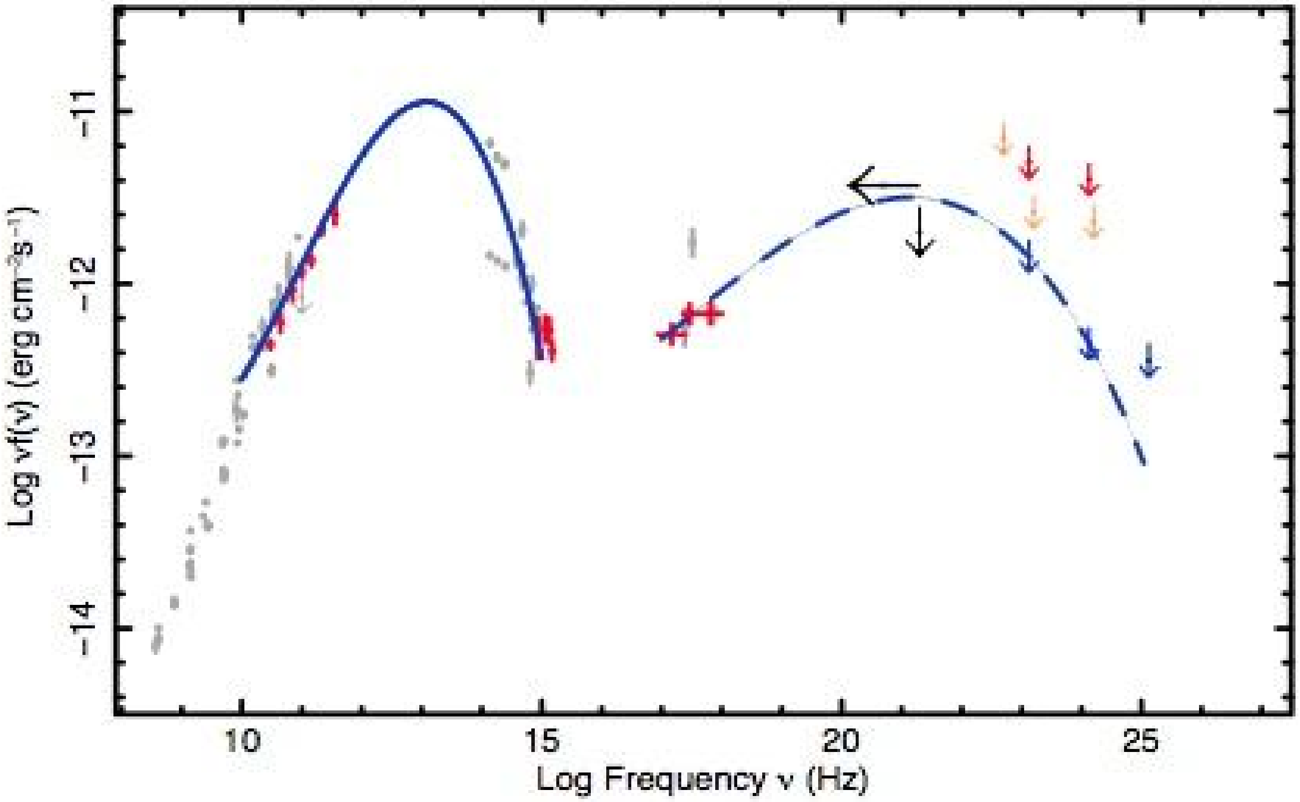

Fig. 10. The SED of the blazar PKS0003-066 as an example of estimation of the upper limits on $\nu^{\mathrm{IC}}_{\mathrm{peak}}$ and on $\nu^{\mathrm{IC}}_{\mathrm{peak}}F(\nu^{\mathrm{IC}}_{\mathrm{peak}})$ combining the X-ray data with the 27 month *Fermi*-LAT upper limits.

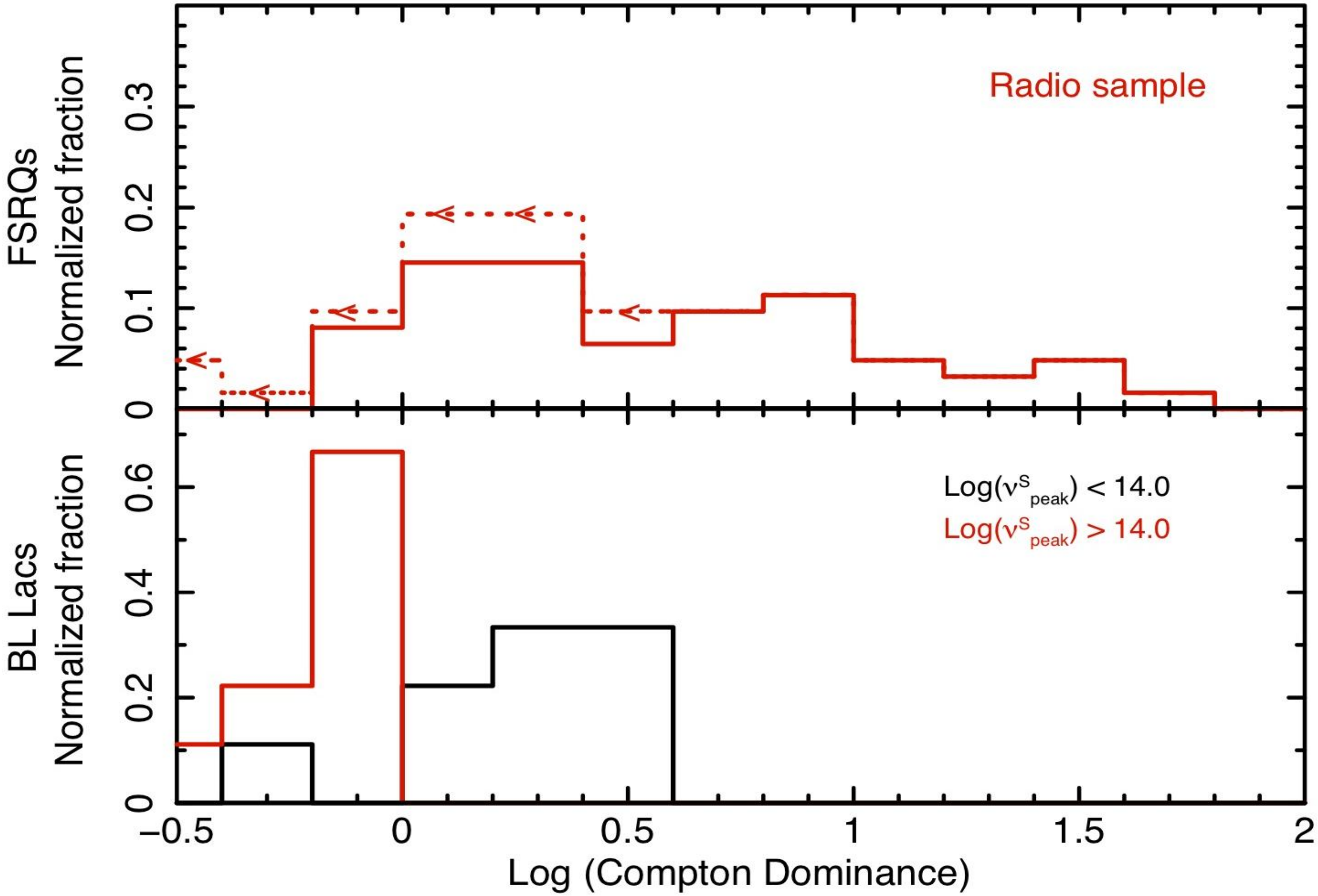
Radio sample
FSRQs
Normalized fraction
BL Lacs
Normalized fraction
Log(ν^{S}_{peak}) < 14.0
Log(ν^{S}_{peak}) > 14.0
Log (Compton Dominance)
0
0.1
0.2
0.3
0
0.2
0.4
0.6
−0.5
0
0.5
1
1.5
2

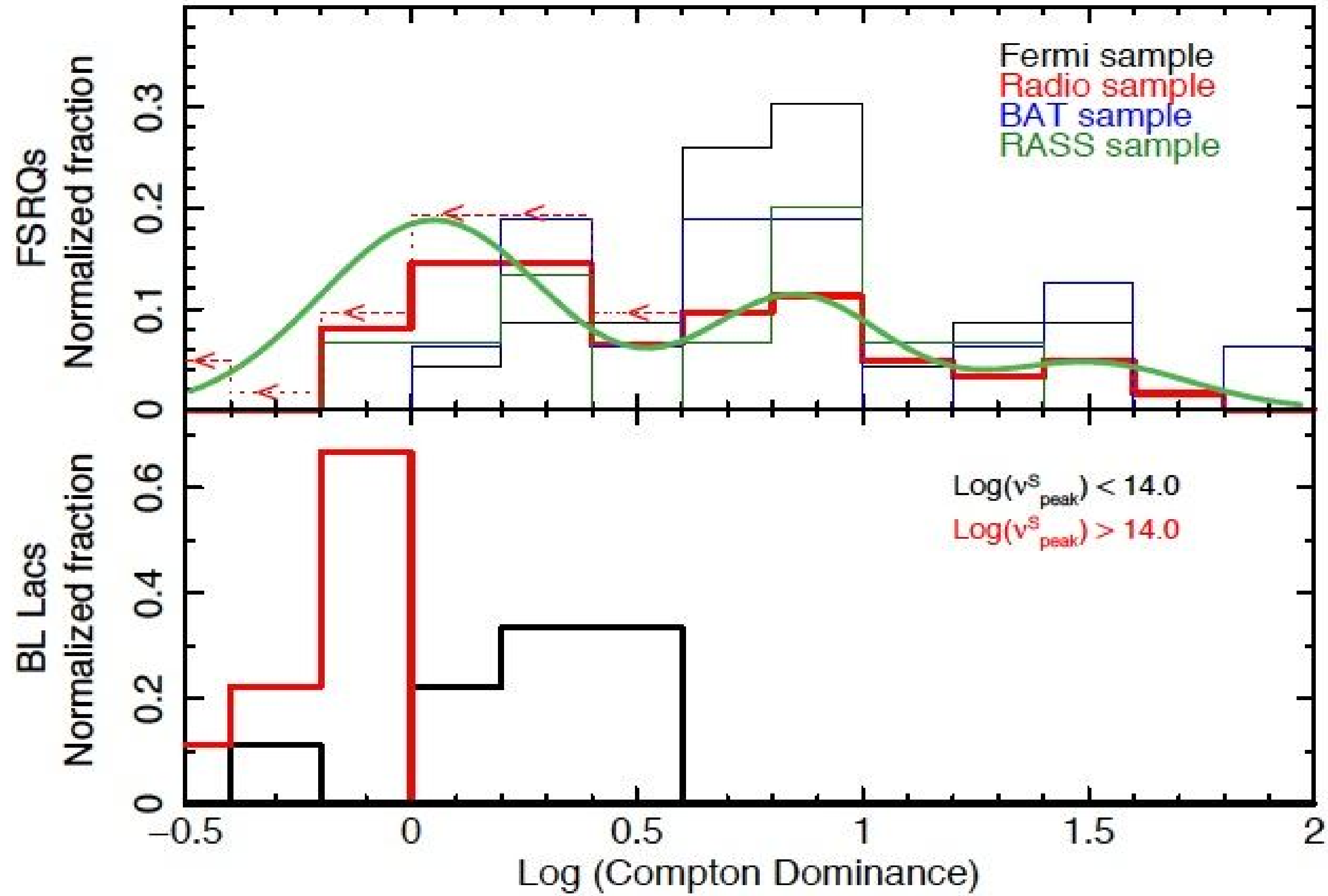

Most (radio selected) FSRQs have Compton Dominance ~ 1 (Log(CD) = 0)

The blazar sequence

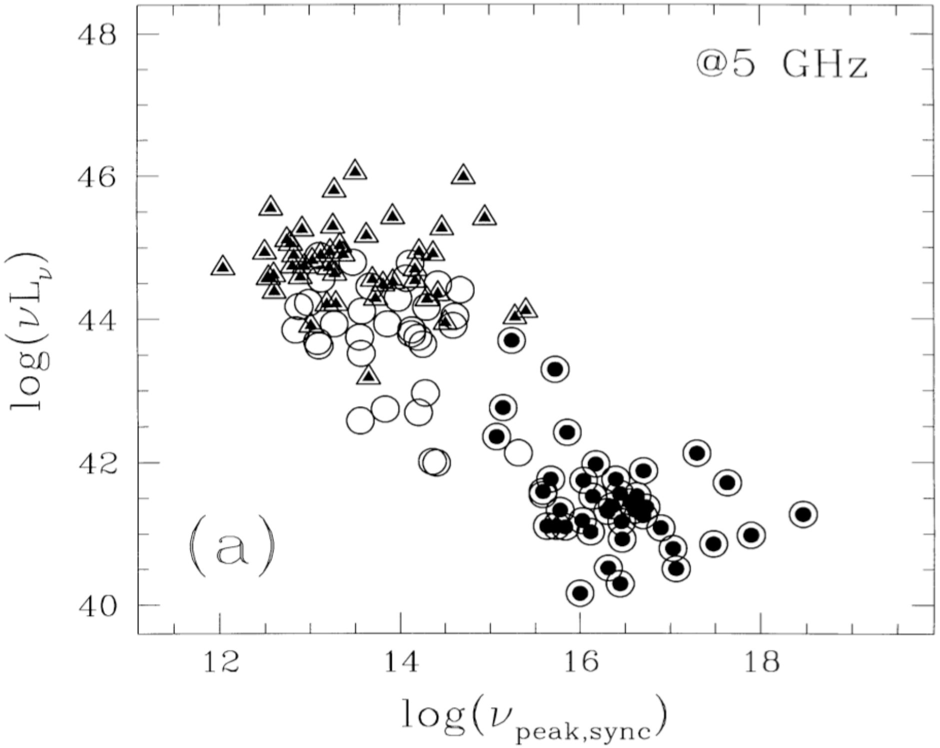

Fossati et al. (1998) MNRAS, 299, 433

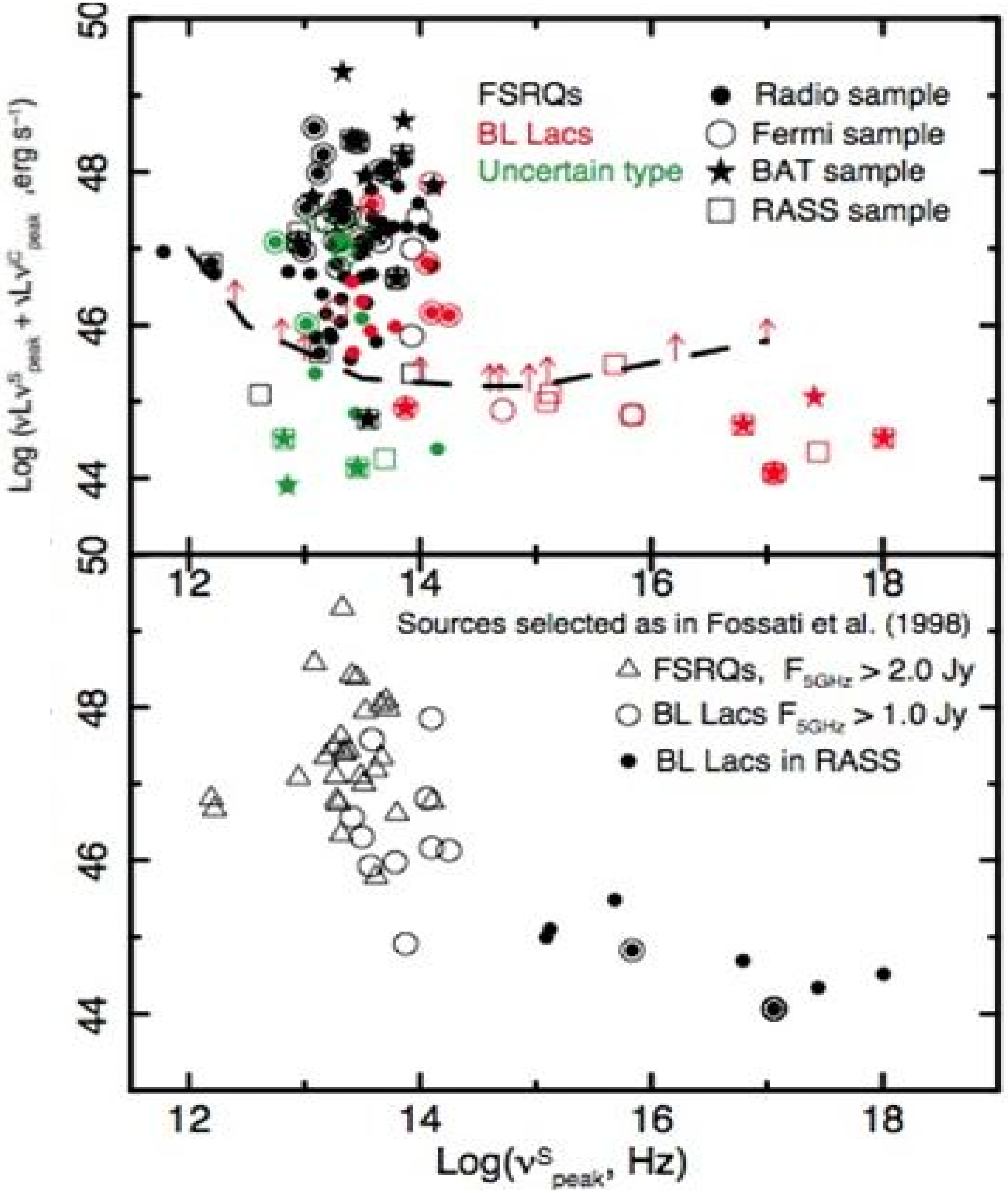

A simplified view of blazars: clearing the fog around long-standing selection effects

P. Giommi[1*], P. Padovani[2], G. Polenta[1,3], S. Turriziani[1], V. D'Elia[1,3], S. Piranomonte[3]
[1] *ASI Science Data Center, c/o ESRIN, via G. Galilei, 00044 Frascati, Italy*
[2] *European Southern Observatory, Karl-Schwarzschild-Str. 2, D-85748 Garching bei München, Germany*
[3] *INAF-Osservatorio Astronomico di Roma, via Frascati 33, I-00040 Monteporzio Catone, Italy*

MNRAS, in press arXiv:1110.4706

Monte Carlo Simulations: The ingredients

- Luminosity function + Evolution estimated from WMAP blazars
- Unified schemes
- Non-thermal component: SSC with single distribution of electron peak energies and Doppler factors
- Thermal component + broad lines from SDSS template
- EW distribution from radio quiet QSOs (estimated from SDSS spectra)
- Disk to jet power ratio estimated from the SED a large number of blazars
- Host Galaxy: Giant elliptical

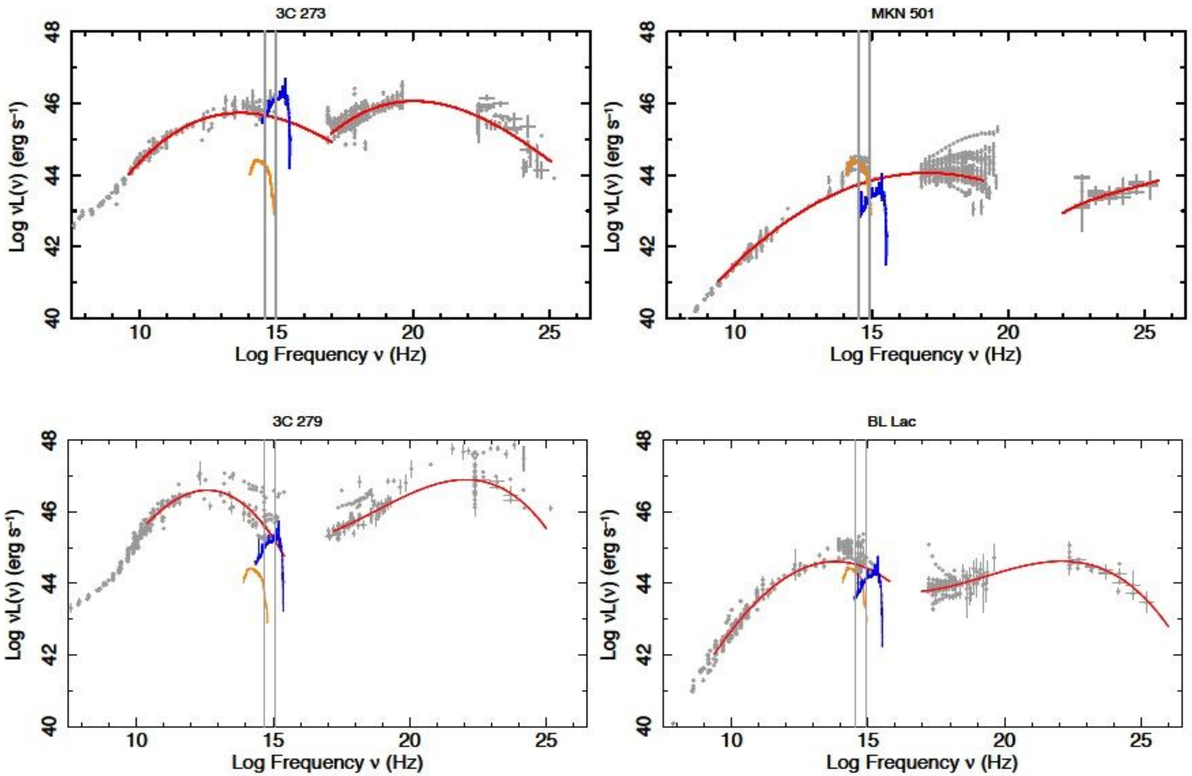

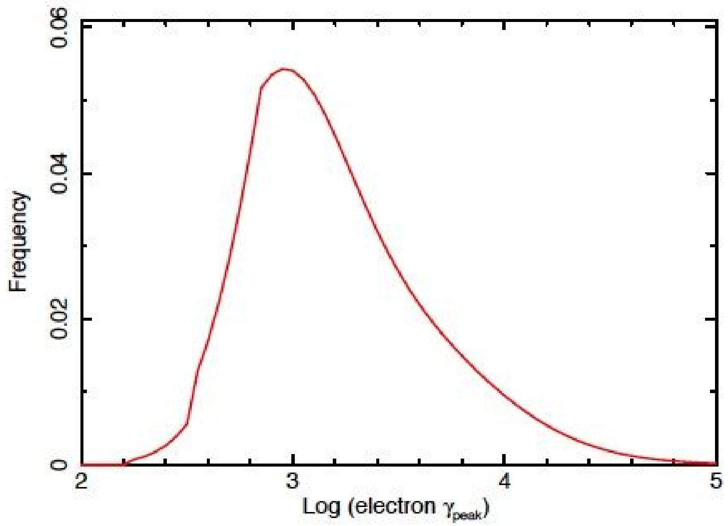

Figure 4. The distribution of the Lorentz factors of the electrons radiating at the peak of the synchrotron SED used for the simulation, which also assumes a magnetic field of B=0.15 Gauss and a gaussian distribution of Doppler factors with $\langle\delta\rangle$=15.

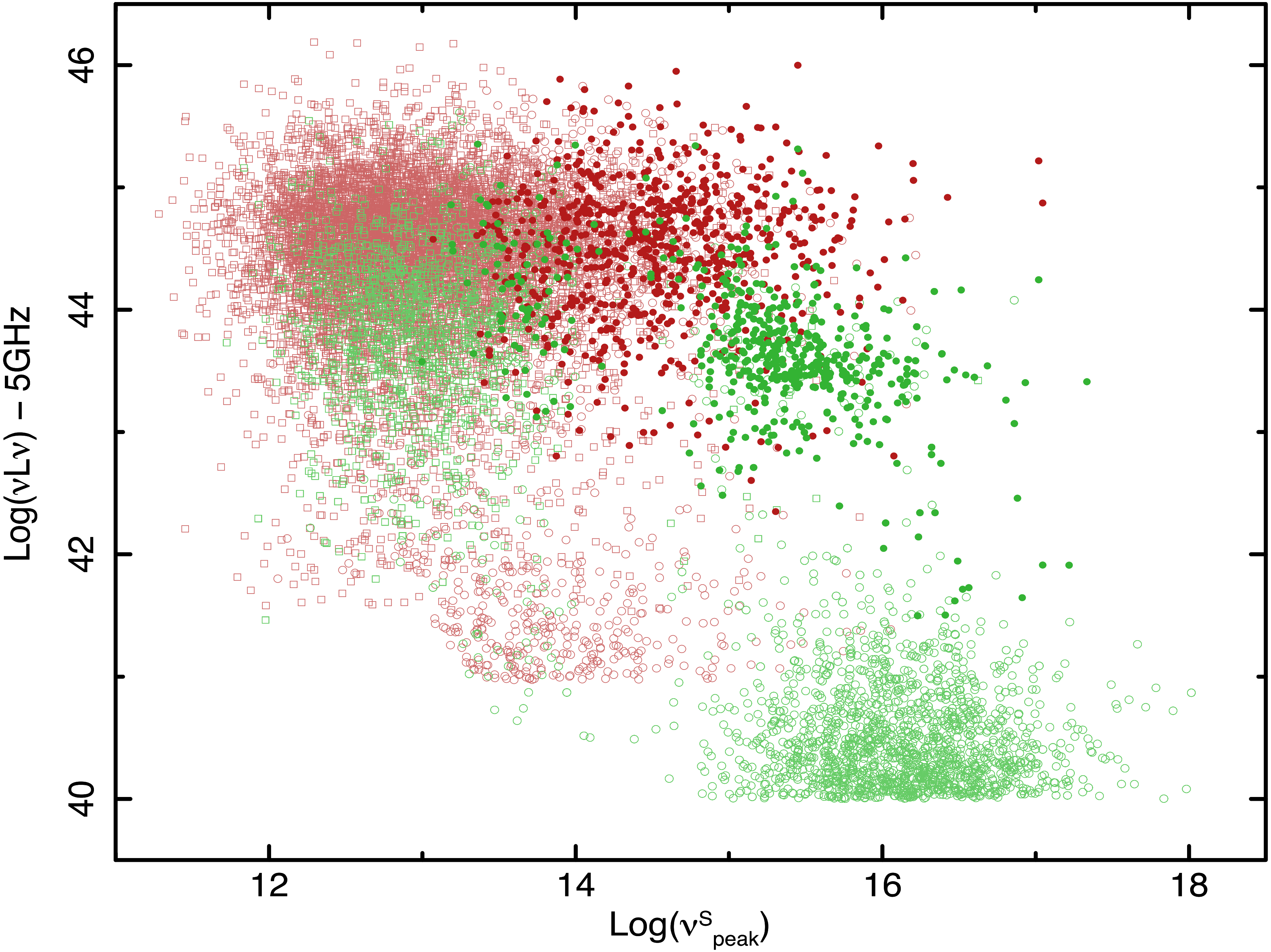

46
44
42
40
Log(νLν) – 5GHz
12
14
16
18
Log(ν^S_peak)

BL Lacertae objects beyond redshift 1.3 - UV-to-NIR photometry and photometric redshift for Fermi/LAT blazars

A. Rau,[1], P. Schady,[1], J. Greiner[1], M. Salvato[2,3], M. Ajello[4,5], E. Bottacini[4], N. Gehrels[6], P. M. J. Afonso[1,7], J. Elliott[1], R. Filgas[1], D. A. Kann[8], S. Klose[8], T. Krühler[1,3,9], M. Nardini[1,10], A. Nicuesa Guelbenzu[8], F. Olivares E.[1], A. Rossi[8], V. Sudilovsky[1], A. C. Updike[11], and D. H. Hartmann[12]

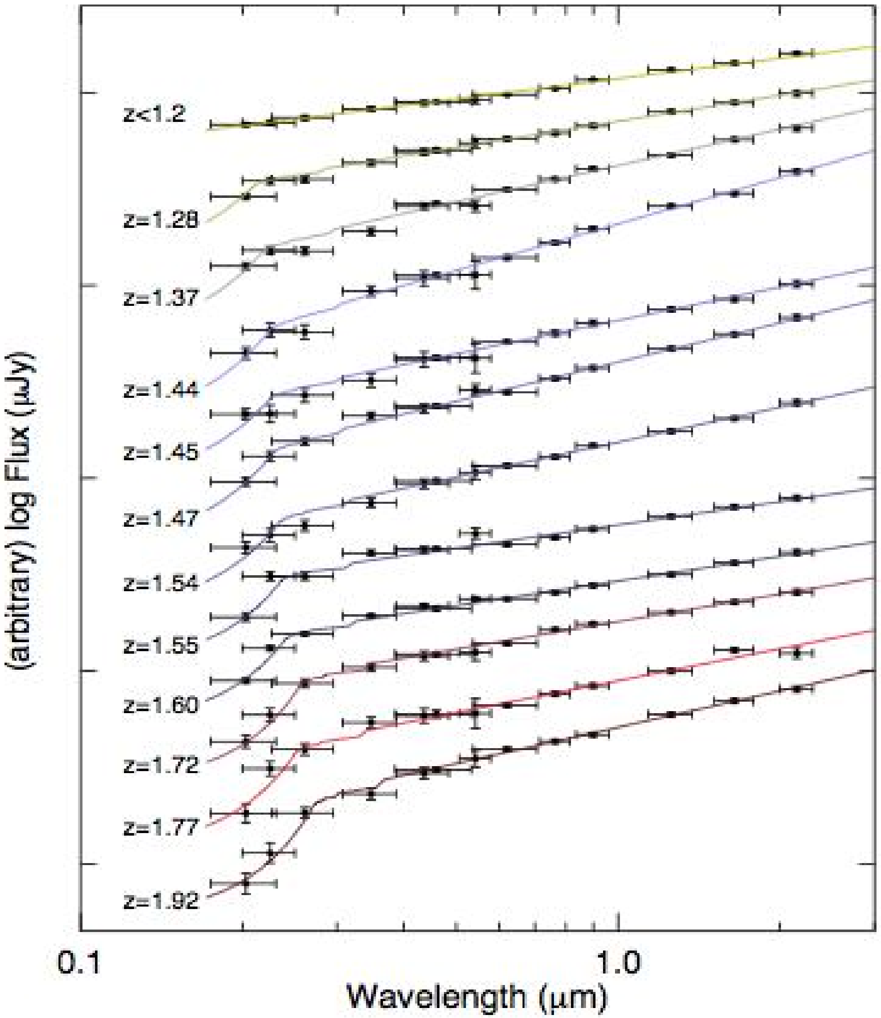

A&A 2012, 538, 26, arXiv1112.0025

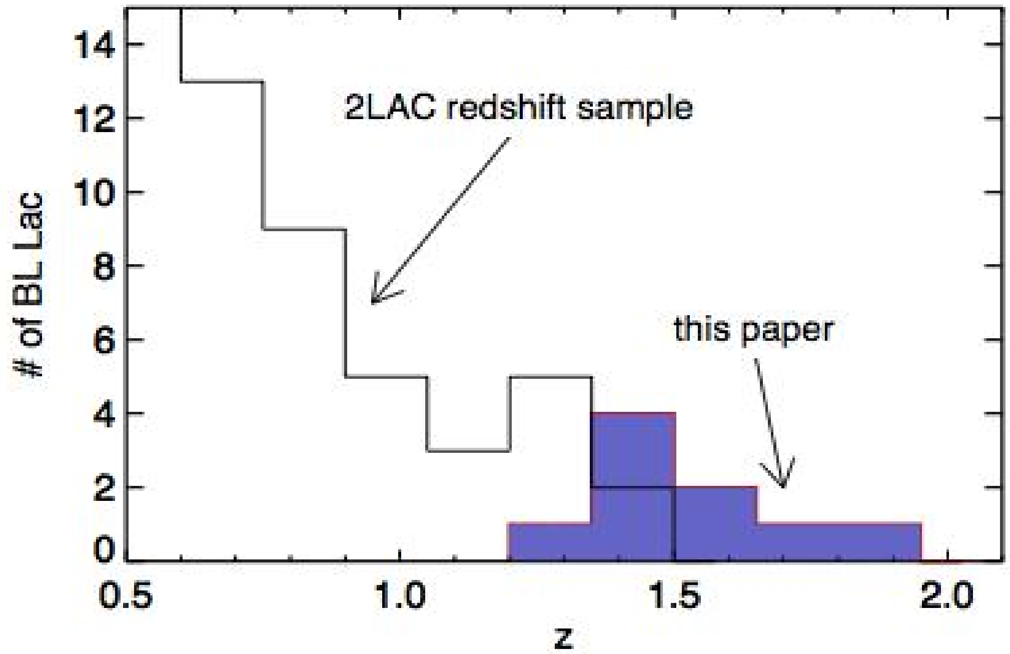

The discovery of high power – high synchrotron peak blazars

MNRAS, in press,arXiv:1202.2236

P. Padovani[1*], P. Giommi[2], and A. Rau[3]

[1] *European Southern Observatory, Karl-Schwarzschild-Str. 2, D-85748 Garching bei München, Germany*
[2] *ASI Science Data Center, c/o ESRIN, via G. Galilei, I-00044 Frascati, Italy*
[3] *Max-Planck-Institut für Extraterrestrische Physik, Giessenbachstr. 1, D-85748 Garching bei München, Germany*

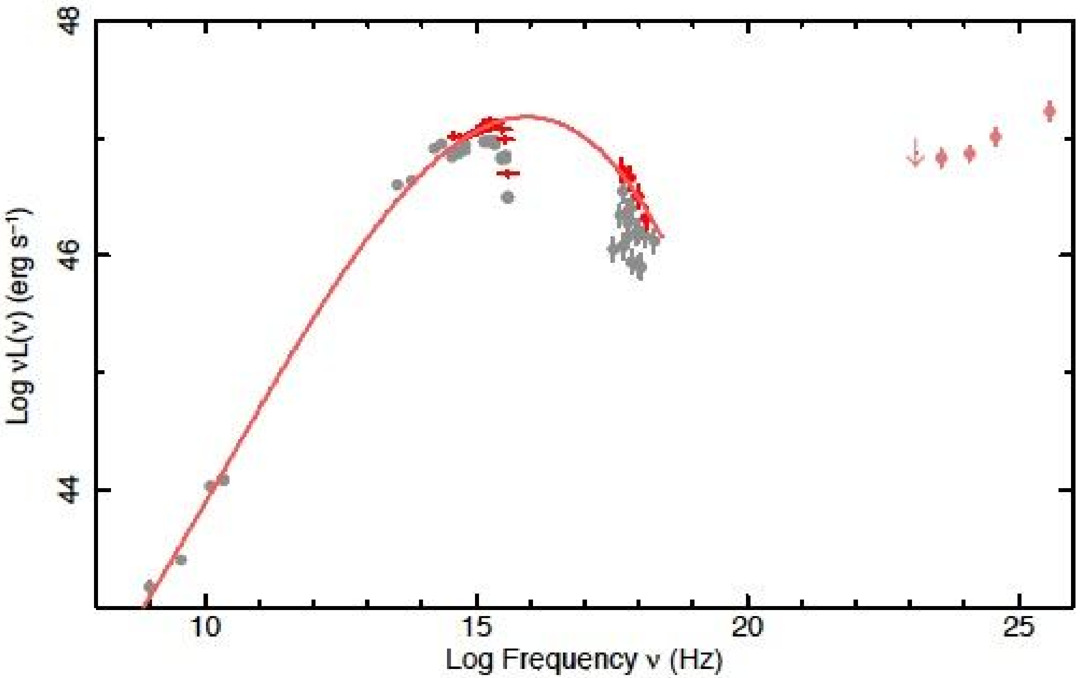

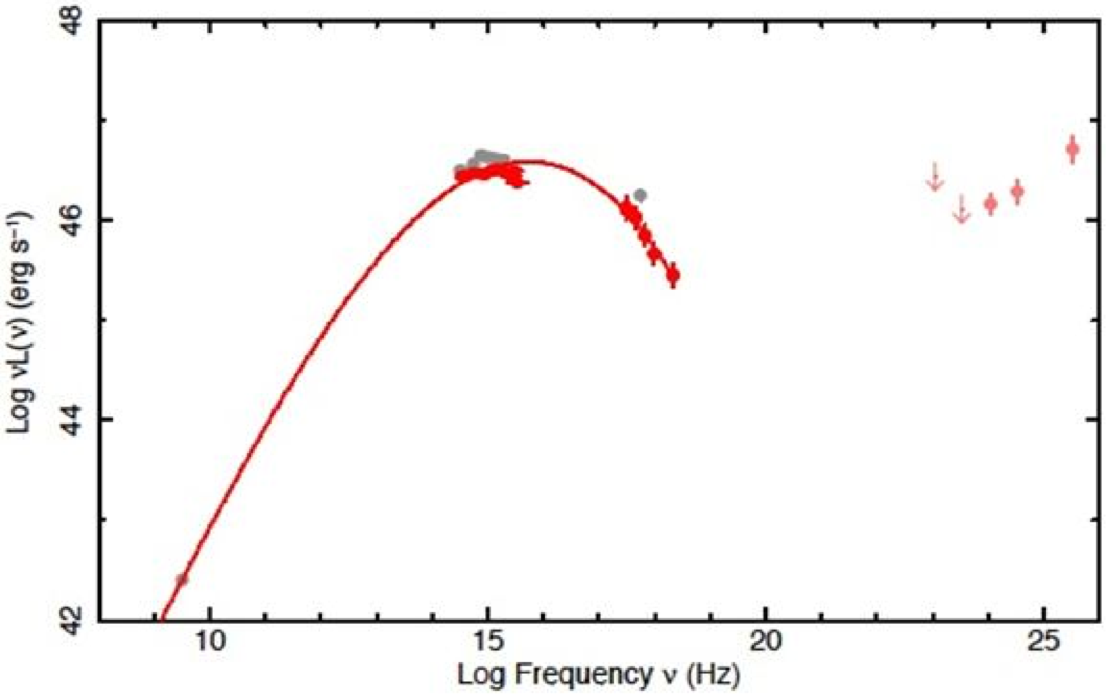

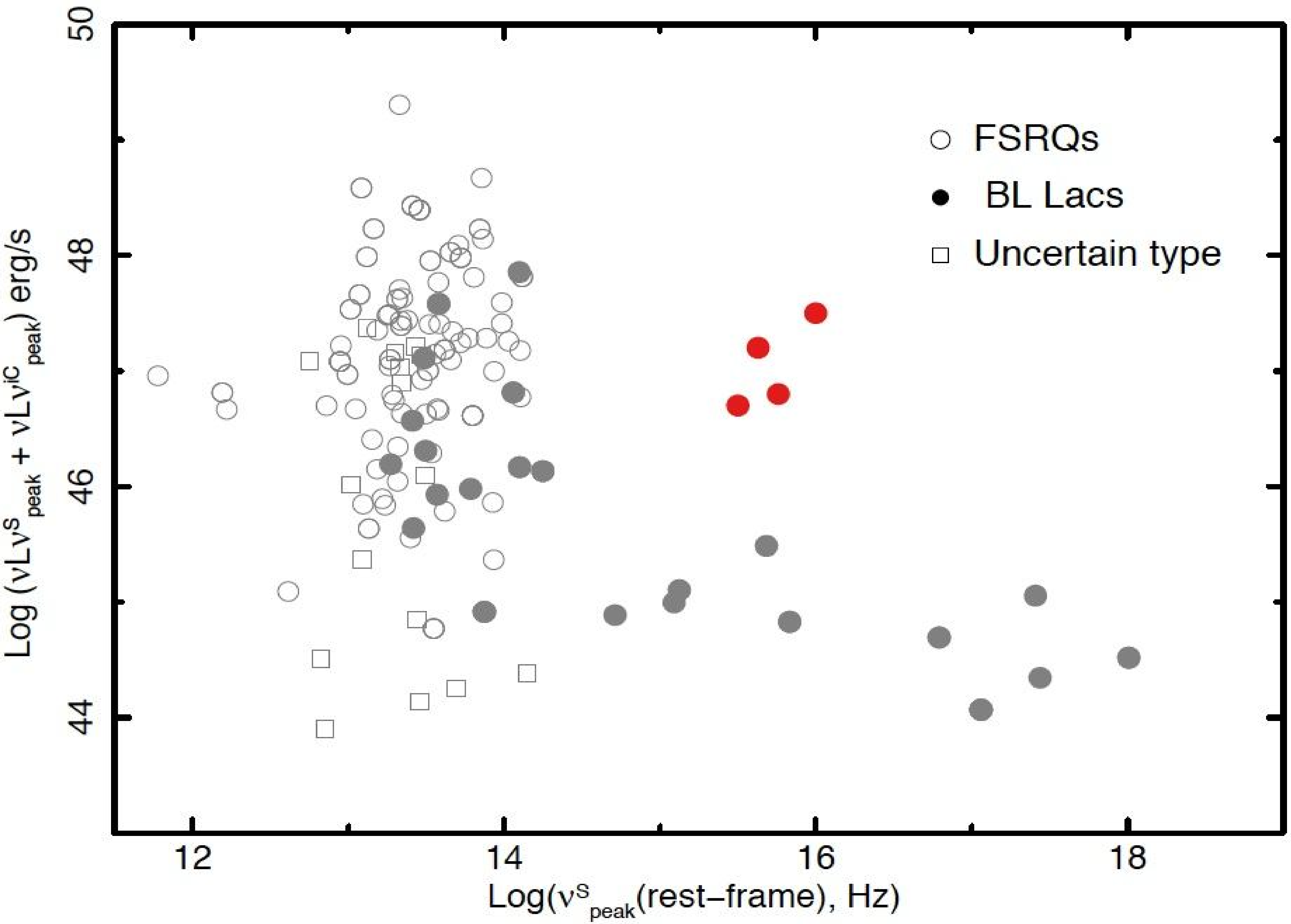

FSRQs
BL Lacs
Uncertain type
50
48
46
44
12
14
16
18
Log ($\nu L\nu^{S}_{peak} + \nu L\nu^{iC}_{peak}$) erg/s
Log(ν^{S}_{peak}(rest–frame), Hz)

Main conclusions

- A lot of progress has been made recently on blazar research thanks to the availability of multi-frequency data from several facilities (Planck, Swift, Fermi, TeV/Cherenkov telescopes, other ground based observatories, etc.)
- The distributions of several blazar key physical parameters have been measured and correlations have been investigated.
- The Compton dominance of (radio selected) blazars peaks at values close to 1 and it extends to values as large as 100 or more.
- Selection effects play a major role in the composition of blazar samples and cause large biases in the estimation of several parameters
- Simple SSC one-zone models are not consistent with the SED of LBL blazars, but might be consistent with the SED of HSP objects
- Simulations show that *all blazar properties* can be interpreted within a *very simple scenario* where classification in different subclasses and their peculiar evolution is the result of the combination of different components and to selection effects.
- High redshift HSP objects have been discovered, these objects are “forbidden in the Blazar sequence scenario”.
- Some distant (up to ~1.6-1.8) HSP blazars detected in the 10-100 GeV band impling that many sources of this type could be detected in future VHE experiments, partivularly the CTA.

Blazar classification

A simulated source is classified as FSRQ, BL Lac or radio galaxy on the basis of the balance of Thermal, Blue-bump/broad-lines, non-thermal/jet radiation and host galaxy in the optical band (3800-8000 Å in the observer frame)

- **FSRQ** if the rest-frame EW (Non-thermal + Blue bump) of any line in the optical band is > 5 Å
- **BL-Lac** if the observed EW (Non-thermal + Blue bump) of any line in the optical band (observer frame) is < 5 Å
- **Radio Galaxy** if only absorption features form the host galaxy are in the optiacal band and Ca H&K break > 0.4

Redshift of BL Lacs is assumed to be ***not measurable*** if the EW of the brightest line in the optical band is < 2 Å

Results

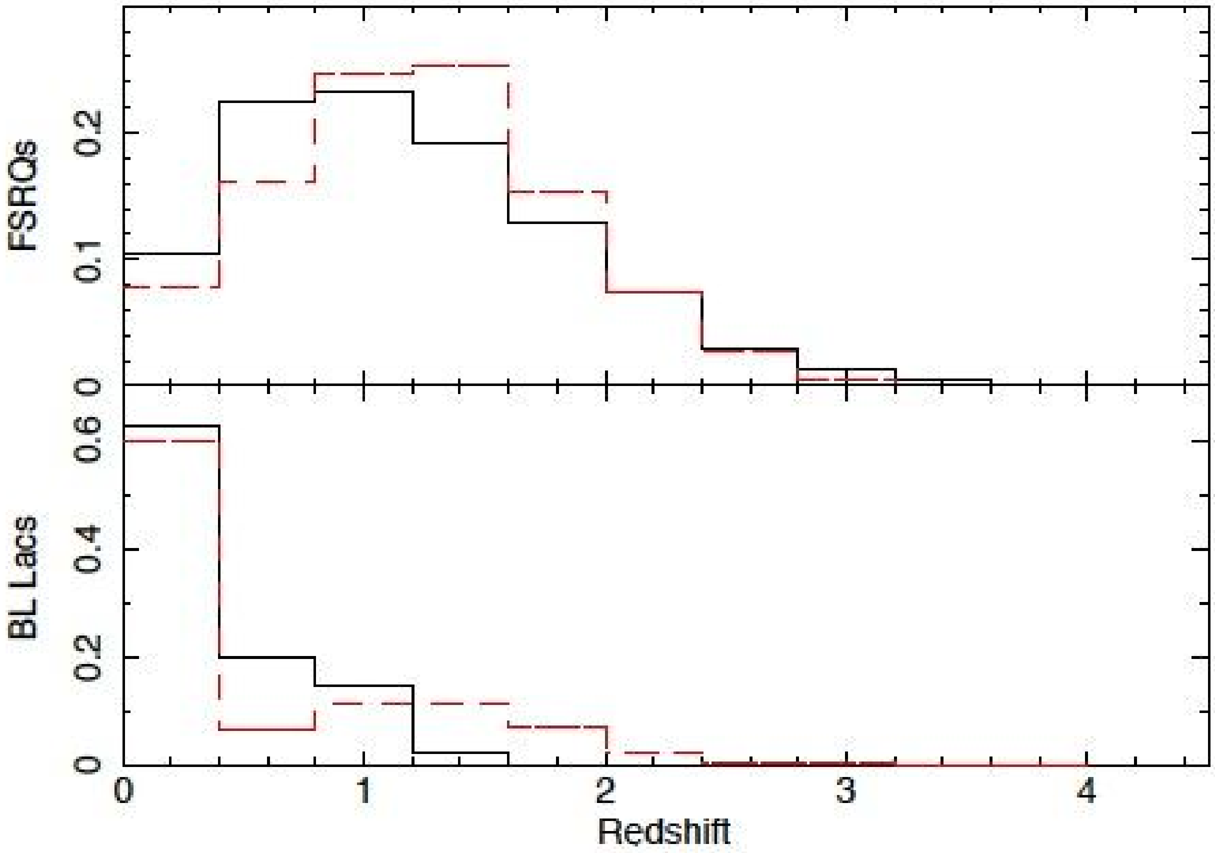

Figure 6. Top panel: the redshift distribution of the WMAP5 FSRQs (solid histogram) compared to that of FSRQs in a simulation of a radio survey (dashed histogram). Bottom panel: the redshift distribution of the WMAP5 BL Lacs (solid histogram) compared to that of BL Lacs in a simulation of a radio survey (dashed histogram)

Results

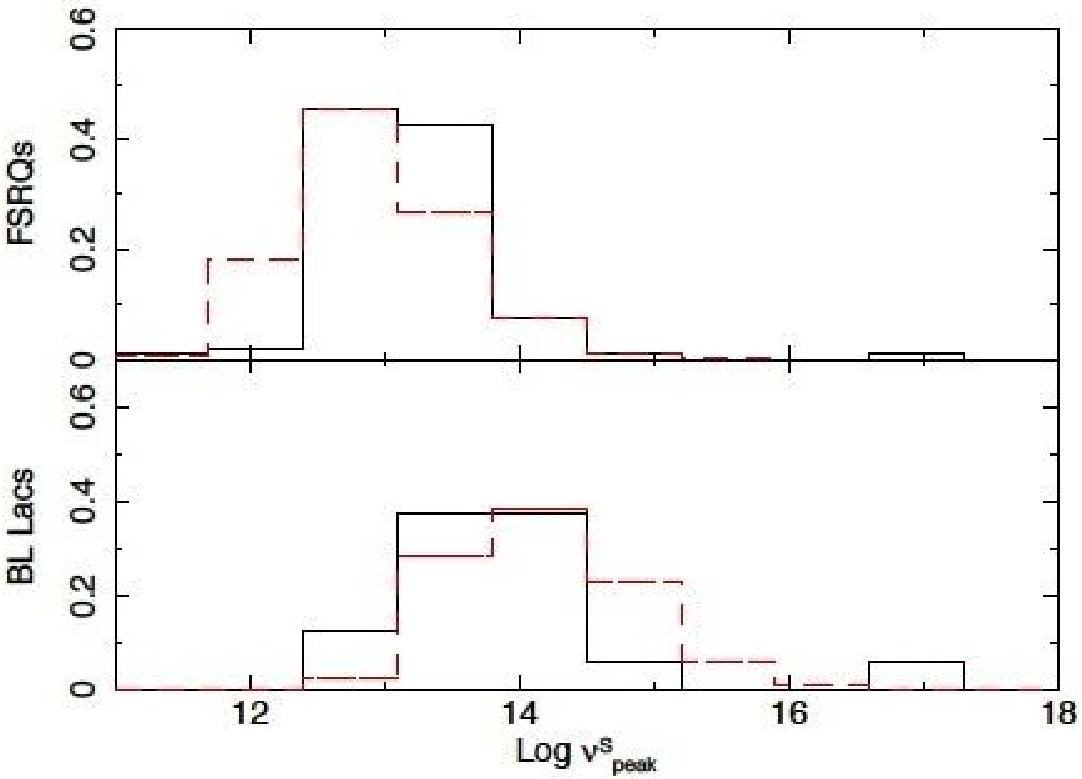

Figure 8. Top panel: the $\nu^{S}_{\rm peak}$ distribution of radio selected FSRQs taken from the work of Giommi et al. (2011) (solid histogram) compared to that of FSRQs in a simulation of a

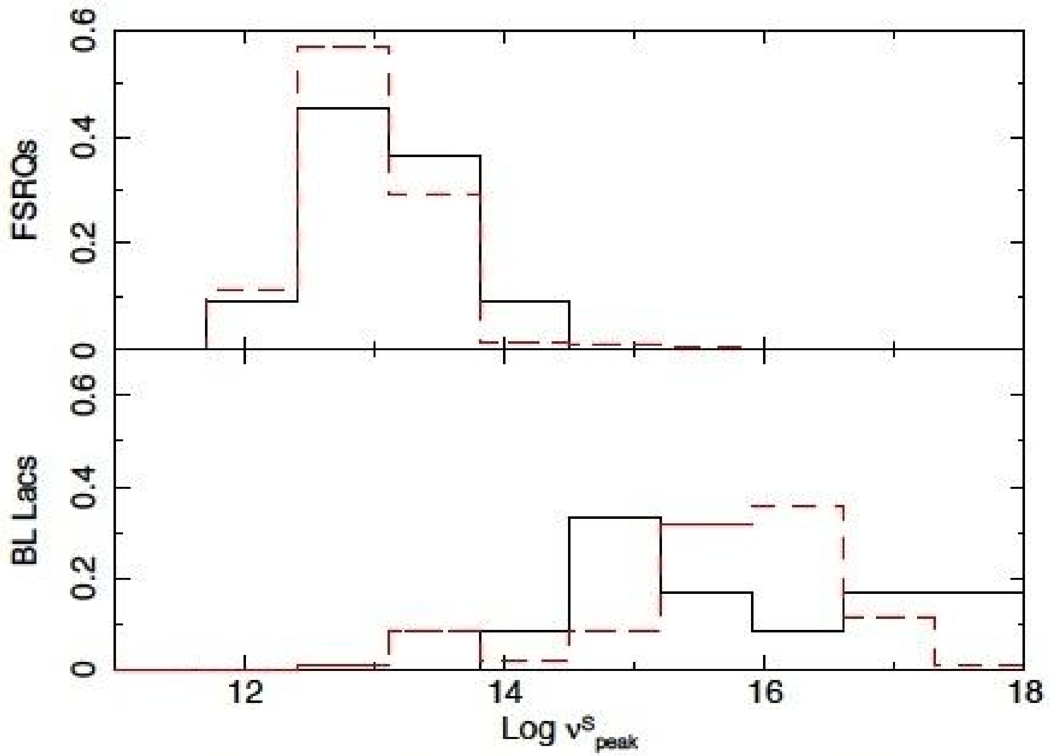

Figure 10. Top panel: the $\nu^{S}_{\rm peak}$ distribution of the X-ray selected FSRQs in Giommi et al. (2011) (solid histogram) compared to that of FSRQs in a simulation of an X-ray survey

The different synchrotron peak energy distributions in BL Lacs and FSRQs is NOT due to cooling or other physical reason, but to selection effects!